## Response to Reviewers comments.

We would like to thank the reviewers for their time and helpful comments. We believe the changes we have made in response to the specific points raised have improved the paper.

We also thank both reviewers for noting the value of our dataset to studies in the region and the atmospheric community. However, we were disappointed that we did not communicate effectively the "new and important information" contained in the paper to reviewer 1 and that reviewer 2 labelled the work "a data description report". We respectfully point out that our paper presents a comprehensive dataset from an interesting new location which uniquely permits airmass contrasts from eastern and western Europe. It also includes state of the art trajectory modelling analysis innovatively coupled with measurements to empirically assess marine deposition rates for the first time for selected OVOC, a comparison to a chemical modelling analysis for the site to assess dominating processes, and comparisons to earlier measurements to address long term regional changes. Furthermore a new analysis separating the data into periods during which the measurement site was either within the planetary boundary layer or within the residual layer/free troposphere was added to the revised version. As such we do believe the paper does contain new information relevant for the readers of Atmospheric Chemistry and Physics and hope that with the revised version, including the suggestions of the reviewers, the value of this paper to our community will become clearer.

Our response to the specific points raised are given below in blue after the reviewer´s remarks (*in italics*).

## Reviewer comments:

## Referee 1

*Several concerns and specific suggestions of the paper are:*
*1. Local anthropogenic emissions: for a population of 1.15 million, it might be worth to explore the importance of local emissions on the VOC levels. Could the high correlations of VOC vs CO (and aromatics) give some insights?*

The location of this campaign was carefully chosen to be close to the upwind west coast of Cyprus (<10km from the sea), on a remote hilltop, in a sparsely populated area to minimize local anthropogenic influence. The prevailing winds advected airmasses from the west (Western Europe) and north (Eastern Europe) over several hundred kilometers of sea and then over the short stretch of land between coast and site. The nearest conurbation was the small village of Polis, which is located to the northeast of the site, with only 1975 inhabitants and negligible influence on our data. Although the island of Cyprus does have over 1 million inhabitants, they do not influence our data, rather our data represent the photochemically processed air from Eastern and Western Europe.
We add the following sentence to make this clearer in the text.

"Although Cyprus has a population of over 1 million their emissions do not influence this dataset since no Cypriot cities or industries lie upwind of the site. Instead the measurements analyzed here represent the transported and photochemical processed pollution emerging from Eastern and Western Europe."

*2. The title doesn't reflect what is told from the manuscript. It stated 'photochemically aged air' but the manuscript doesn't provide any analysis on this matter.*

We are somewhat confused by this comment. As our introduction clearly states our campaign location was carefully chosen to be in a position to measure photochemically processed air emerging from Eastern and Western Europe. This is in contrast to the majority of atmospheric chemistry campaigns which tend to be positioned close to a source (e.g. in a megacity or a forest). The FLEXPART model which we have used extensively in this study (see for example figures 9,12) shows transport times from the continental emission sources which are a minimum of 12 hours from Eastern Europe and a minimum of 2 days from Western Europe. During this time the air was photochemically processed (by OH and photolysis from the intense Mediteranean sunlight.) The extremely low NOx values measured during the campaign are also indicative of very aged air.
We therefore think that the title does reflect exactly the reality of the campaign and choose to retain it. However, in order to make this point clearer we have amended the abstract to read
"The Lagrangian model FLEXPART was used to determine transport patterns and photochemical processing times (between 12 hours and several days) of air masses originating from source regions in Eastern and Western Europe."
In addition we now add to the introduction the sentences,
"This study was designed to investigate the chemical characteristics of polluted air emerging from the European continent which is then photochemically processed over the Mediterranean Sea between 12 hours and several days en-route to the island of Cyprus. It is therefore in contrast with most atmospheric chemistry campaigns that generally investigate source impacted locations (e.g. in forests and megacities)."

*3. Abstract: loss rates: significant digits should be consistent for all reported numbers. These numbers all seem very small. Are they important?*

The reviewer is correct to question this formatting, thanks. In the course of the new analysis, loss rate constants are calculated and given as follows:

"Methanol and acetone decreased with residence time in the marine boundary layer (MBL) with loss rate constants of 0.031 ± 0.004 $h^{-1}$ and 0.022 ± 0.003 $h^{-1}$ from Eastern Europe and 0.029 ± 0.005 $h^{-1}$ and 0.014 ± 0.003 $h^{-1}$ from Western Europe, respectively."

These numbers are important and interesting, because they represent the determined net loss over the ocean which is the result of several processes such as dilution, photochemical degradation, uptake or emission by the ocean and production from the oxidation of larger organic molecules.

*4. Introduction (and its references) should be updated to reflect some newest developments on their global budgets particularly for methanol and acetone. More regional studies for this area should be cited otherwise I don't really see the motivations of this study.*

At the time of submission we thought we had faithfully accredited all relevant published previous work. While reviewer 1 does not give any information on overlooked references, we are grateful to reviewer 2 to pointing out the Müller et al reference which was published shortly after our last literature review. We have also since found a new relevant reference Khan et al. (2015) concerning the global budget of acetone. Both these references are now included in the text discussion.

"According to Fischer et al. (2012) the global acetone budget sums up to 146 Tg $yr^{-1}$, 32 Tg $yr^{-1}$ being terrestrial emissions from biosphere and 31 Tg $yr^{-1}$ being photochemical production (26 Tg $yr^{-1}$ from isoalkanes, mainly anthropogenic, 5 Tg $yr^{-1}$ biogenic). The main acetone sinks are photolysis and reaction with OH: Fischer et al. (2012) report a loss of 33 Tg $yr^{-1}$ by OH oxidation and 19 Tg $yr^{-1}$ by photolysis from a total sink of 146 Tg $yr^{-1}$. Depending on the season and geographical location the ocean can either be a sink (82 Tg yr-1) or a source (80 Tg yr-1) of acetone (Fischer et al., 2012). Khan et al. (2015) on the other hand calculate a global acetone source of 72.7 Tg $yr^{-1}$, of which 55.6 Tg $yr^{-1}$ are photochemical production from $\alpha$-pinene, $\beta$-pinene and propane and 17.1 Tg $yr^{-1}$ direct emission. From the total sink of 72.9 Tg $yr^{-1}$ 30.8 Tg $yr^{-1}$ represent OH oxidation, 30.3 Tg $yr^{-1}$ photolysis and 11.8 Tg $yr^{-1}$ dry deposition and the ocean is regarded as being globally in a near equilibrium state (Khan et al., 2015). A global acetone source of 95 Tg $yr^{-1}$ was given by Jacob et al. (2002). The main contributions are emissions by terrestrial vegetation (33 Tg $yr^{-1}$), by the ocean (27 Tg $yr^{-1}$) and the oxidation of isoalkanes (21 Tg $yr^{-1}$). Jacob et al. (2002) determined a sink by OH reaction of 27 Tg $yr^{-1}$ and by photolysis of 46 Tg $yr^{-1}$ from a total loss of 95 Tg $yr^{-1}$."

And for methanol

"Methanol is primarily emitted from plants (Galbally and Kirstine, 2002), with a relatively small photochemical production term in the estimated global budget, 37 Tg $yr^{-1}$ from a total of 242 Tg $yr^{-1}$ found by Millet et al. (2008). However, recent model calculations by Müller et al. (2016) revealed that the photochemical reaction between methyl peroxy and hydroxyl radicals is, depending on the region, a significant source of methanol. The reaction was found to result in 115 Tg $yr^{-1}$ of methanol, which is in the range of the global terrestrial emissions. For example Millet et al. (2008) list a methanol source from terrestrial plant growth of 80 Tg $yr^{-1}$ and from plant decay of 23 Tg $yr^{-1}$. One of the main sinks of methanol is the oxidation by OH, while the role of the ocean is not completely characterized: Millet et al. (2008) report a methanol sink via OH oxidation of 88 Tg $yr^{-1}$ of a total sink of 242 Tg $yr^{-1}$. Furthermore Millet et al. (2008) state an oceanic source of 85 Tg $yr^{-1}$ and an oceanic sink of 101 Tg $yr^{-1}$ which results in a net sink of 16 Tg $yr^{-1}$. Jacob et al. (2005) found a loss of methanol via the reaction with OH of 129 Tg $yr^{-1}$ and an oceanic net sink of 10 Tg $yr^{-1}$ from a total sink of 206 Tg $yr^{-1}$."

Regarding the last sentence in this comment "*More regional studies for this area should be cited otherwise I don't really see the motivations of this study.*"
We are again somewhat confused by this comment. Does the reviewer really mean to say that in his/her opinion measurements are only worth doing in regions where measurements already exist? The measurements we present here are new, taken in an interesting location downwind of the European continent where the air from two distinct locations is extensively photochemically processed prior to measurement. Where available we do compare with previous regional studies conducted in the Mediterranean marine boundary layer (e.g. measurements made on Crete) in order to deduce longer term trends, but what we present here is a brand new comprehensive dataset that is analyzed to develop new perspectives on the atmospheric chemical processing of OVOC.

*5. Humidity dependent instrument sensitivity: a. Only two calibrations were performed: beginning and end of the campaign, but the humidity seems to vary a lot during the campaign. It is unclear how humidity was accounted for the measurements. Given some conclusions are related to the variability of ambient humidity, authors should be very careful on their observation's dependence on RH. b. The paper also commented that instrument sensitivity for methanol and isoprene didn't show any humidity dependency. Why is that? It seems PTR methanol sensitivity has a strong dependence on RH. c. One simple check on the RH effect is to examine if the background signal changed a lot during the campaign.*

a) The reviewer is correct to address the humidity dependence of the calibrations given the strong variations of RH experienced during the campaign.

"At the beginning and at the end of the campaign a comprehensive 4 point calibration of the instrument (spanning the measured range of compounds) was performed at 4 and 3 different humidities, respectively. The humidity level was determined by using the ratio between the isotope of the water cluster and the isotope of the primary ion and this ratio lay between 0.07 and 0.3 for the different calibrations. These values correspond approximately to a range of 25% to 80% relative humidity. A commercial gas standard (Apel-Riemer Environmental) containing 14 compounds was used. Great care was taken to account for this humidity dependence in each datapoint. The sensitivity of the instrument for each individual data point was derived from a linear interpolation over time between the two calibrations and corrected for the co-measured ambient relative humidity at that time. The decrease in sensitivity between the two calibrations (2.5 weeks apart) were generally modest, ranging from 10% (e.g. isoprene) to 23% (e.g. methanol)."

The above text is now added to the manuscript to clarify how the measurements were quantified. More specific information about the humidity dependency of acetic acid can be found under comment 2 of referee 2.

b) “Most compounds measured by PTR-TOF-MS show a more pronounced humidity dependence between 0 and ca. 15% relative humidity (whereby dry conditions are most sensitive), but with increasing humidity the dependency weakens so that decreases in sensitivity in the upper humidity range are very small. This behavior which was described by an exponential fit function was observed for all compounds except isoprene and methanol. Isoprene shows almost no humidity dependency, because its reaction rates with the primary ion and the water cluster have roughly the same value as has been previously reported by Smith et al. (2001). The variations in the sensitivity for methanol did not show the same characteristic exponential behavior described above, so that no interpolation was made. However, since the values showed a variation of only 5-10 %, an averaged calibration factor was used instead. The underlying reason for this anomalous behavior is not known in the case of methanol.”…

…

“During a few periods of the campaign the ambient humidity was below the lower limit of the calibrated humidity range. The absence of a trend for methanol and isoprene precluded interpolation, while the exponential fit for the other compounds is afflicted with a higher error in this range. The variation in sensitivity in the range below 25% relative humidity was estimated from previous measurements in our laboratory and was included in the error calculation. The values of the total uncertainty within the calibrated range varied between 10% (e.g. isoprene) and 23% (e.g. methanol) and increased to a maximum of 28%(methanol) in the low humidity range.”

The above text is now inserted in the revised manuscript.

c) Background variations experienced during the campaign were small and unsuitable for judging humidity dependences. It should be noted though that the background varies not just as a function of humidity but also with instrument noise. Therefore humidity dependent calibrations are the best way to determine this dependency (as we have done). For our quantification we subtract the background corresponding to the measurement time interpolated between background measurements, then apply our humidity dependent calibration factors for each data point (see above).

We believe the text inserted in answer to points a) and b) should make the calibration procedure clearer.

*6. Page 6. Acetic acid measurements: It seems PAA measurements were not subtracted from the PTR 61.0284 amu. Would the main conclusion change if such subtraction were attempted?*

A fraction of the PAA data was not subtracted from the 61.0284 signal because the PAA signal was only measurable during a small portion of the campaign with very low counts-per-second (ca. 0.3). It´s inclusion would therefore not affect the conclusions. This point was already made in the text, but the text has been amended for clarity in light of the comment, as below.

"The PTR-TOF-MS was not calibrated for PAA and only detected it with low count rates (ca. 0.3 cps) at mass 77.0233 amu for a few days of the campaign. Španel et al. (2003) reported that 90% of protonated PAA can be measured at the exact mass of acetic acid, while 10% are recorded at the mass of the mother ion (77.0233 amu). If this is taken into account, PAA would still influence acetic acid, but between only ca. 10 and 15% because of the low count rates."

*7. Section 2.2.2: So I assume the GC-MS reports speciated monoterpene measurments? Has any attempt done to compare the GC-MS measured vs. PTR measured C2 monoterpene? Are they consistent? Also, more details should be reported for the GC-MS system.*

And

*8. Page 8 Line 253: again here it seems the PTR monoterpene is reported, but later GC-MS data is reported. It is very confusing which dataset is used for the monoterpene analysis.*

The reviewer has suggested comparing the speciated monoterpene results provided by the GC-MS and the total monoterpenes measured by the PTR-TOF-MS. Therefore we now provide this information as described below.

Firstly, the relevant information concerning the GC-MS system is added to the experimental section:

"Isoprene and monoterpenes ($\alpha$-pinene, $\beta$-pinene , $\Delta$-3 carene and limonene) were quantified by a commercial GC-MS system (MSD 5973; Agilent Technologies GmbH) combined with an air sampler and a thermal desorption unit (Markes International GmbH). The sample interval was 45 min, the sampling time amounted to 20 min, while calibrations were carried out every 8-12 samples with a commercial gas standard mixture (National Physical Laboratory, UK). The detection limit was 1-2 pptv and the total uncertainty ca. 15 %. The volatiles were trapped at 30 °C on a low-dead-volume quartz cold trap (U-T15ATA; Markes International GmbH), which was packed with two sorbent beds (Tenax TA and Carbograph I). The trap was then heated to 320 °C and the compounds were transferred to a 30m GC column (DB-624, 0.25mm I.D., 1.4µm film; J&W Scientific). The temperature of the GC oven was programmed to stay stable at 40°C for 5min, thereafter increase to 140 °C with a rate of 5 C/min and finally the rate was increased to 40 °C/min to reach the final temperature of 230 °C, which was held for 3 min. Due to co-elution of $\beta$-pinene and $\Delta$-3 carene, a separation was not possible and therefore the signal was treated as the sum of the two species."

A comparison between the GC-MS and the PTR-TOF-MS data has now been added to the paper and it was made clear which data were reported in each case: the following text was added,

"Isoprene and several different monoterpenes were also measured by a GC-MS system operating at a lower time resolution at the same site. A comparison between the results of the two instruments can be found in the Figures 3 and 4. PTR-TOF-MS data with a 1min time

resolution were merged onto the 20 min sampling time of the GC-MS. The dashed line in these figures refers to a time period where a contamination in the PTR-TOF-MS is assumed. This period was excluded from the comparison. During the day the isoprene data measured by the PTR-TOF-MS were ca. 1.3 times higher than the GC-MS data (Figure 3), while at the low level nighttime values the PTR-TOF-MS system measured ca. 7.5 times more isoprene than the GC-MS (determined from diel median values over the whole campaign). An insufficient determination of the humidity dependency of the PTR-TOF- MS for isoprene can be ruled out as a possible explanation, because isoprene measurements are not dependent on humidity (see section 2.2.1). A correlation of the two datasets (PTR vs. GC data) using a bivariate fit algorithm resulted in a slope of 1.2, an intercept of 10.4 pptv and a $r^2$ value of 0.88. The reason for the discrepancy is yet unknown. The correlation plots between PTR-TOF-MS and GC-MS measurements can be found in the supplement S1. The data were color coded by the date and time of the recording. It becomes clear that the agreement between the two data sets varied slightly with time. Thus, an instrumental issue during a specific period can not be ruled out. The lower part of Figure 4 shows the data of $\alpha$-pinene, the sum of $\beta$-pinene and $\Delta$3-carene as well as limonene measured by the GC-MS system. The sum of the monoterpenes measured by GC-MS are compared to the total monoterpene signal measured by PTR-TOF-MS at 137.13 amu in the upper part. The PTR-TOF-MS data are up to 2.5 times higher than the GC data (determined from diel median values over the whole campaign). This can partly be explained by the fact that the sum on mass 137 amu can also contain monoterpenes other than those quantified by the GC-MS. The correlation between the two signals (bivariate fit algorithm, PTR vs. GC) lead to a slope of 1.6, an intercept of 0.64 pptv and a correlation coefficient $r^2 = 0.80$. This is reasonable given unmeasured monoterpenes by GC-MS. Furthermore, the total monoterpene signal of the PTR-TOF-MS system was calibrated with $\alpha$ -pinene. Thus, slight differences in sensitivity, which occur as soon as $\alpha$ -pinene is not the dominant species, can play a role."

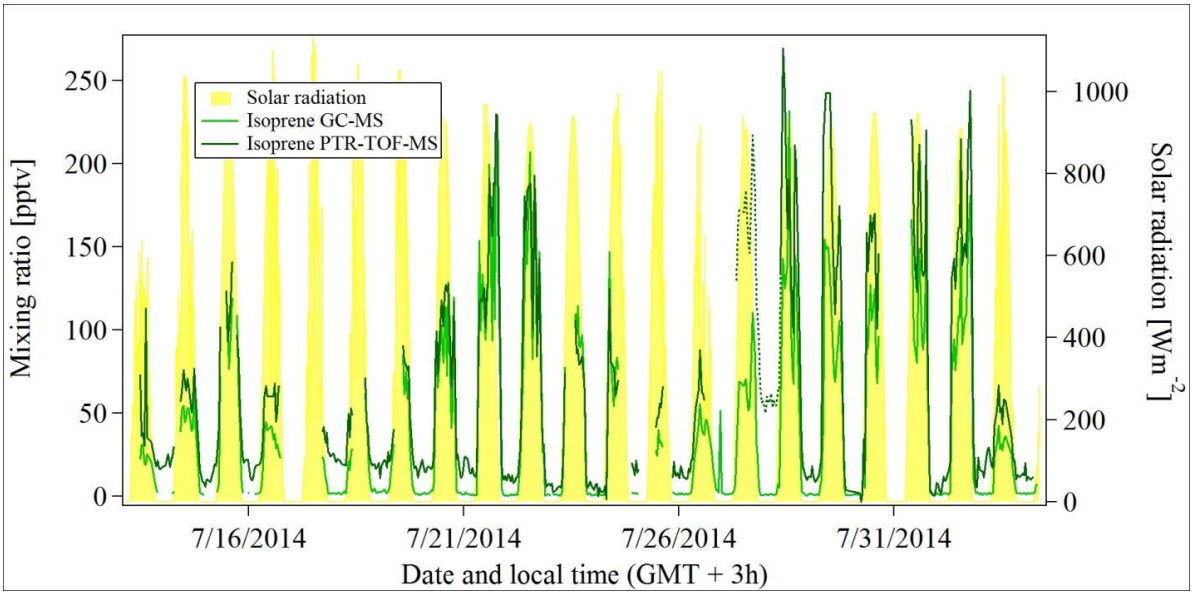


"Figure 3. Time traces of isoprene in pptv measured by GC-MS and PTR-TOF-MS as well as solar radiation in $Wm^{-2}$. The PTR-TOF-MS data with a time resolution of 1 min were merged on the 20 minute sampling time of the GC-MS. Solar radiation is shown in a 10 min time resolution. The dashed line marks a possible contamination in the PTR-TOF-MS data."

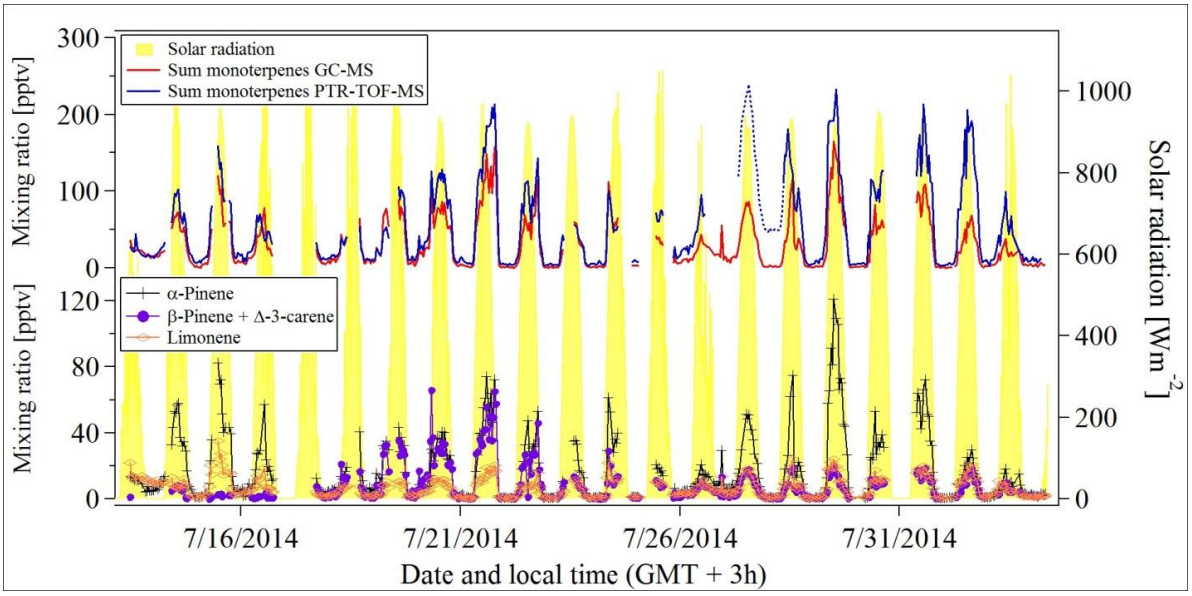


"Figure 4. Time traces of different monoterpenes in pptv as well as solar radiation in $Wm^{-2}$. The PTR-TOF-MS data with a time resolution of 1 min were merged on the 20 minute sampling time of the GC-MS. Solar radiation is shown in a 10 min time resolution. The upper part shows the sum of the monoterpenes measured by GC-MS and PTR-TOF-MS, the lower part displays individual monoterpenes measured by GC-MS, only. The dashed line marks a possible contamination in the PTR-TOF-MS data."

*9. Page 8 line 254: Any particular reasons that the tropical forest region is used to compare the data in Cyprus? The location of the site is 34 degree N, which is at mid-latitude.*

The reason we compared the levels of isoprene and monoterpenes to the tropical forest is to set the current Mediterranean vegetation emission of isoprene and monoterpenes in a wider global vegetation context before making the comparison to previous regional measurements. In order to make this clearer we now amend the text to include a more northerly Boreal forest measurement campaign.
We have amended the text as follows
"This is in contrast to tropical forest regions where typical values of 7.6 ppbv isoprene and 1 ppbv monoterpene have been reported recently (Yañez Serrano et al., 2015) and Boreal forest regions where levels of isoprene and monoterpenes are ca. 100 pptv and 300 pptv respectively (Yassaa et al. 2012). The measured values in this study are consistent with levels reported previously from Mediterranean areas (Liakakou et al., 2007; Davison et al., 2009)."

*10. Section 3.1: I would suggest the authors also take a look at MVK+MACR, since their lifetime is longer than isoprene so they could give a relatively regional perspective on the biogenic emission for Cyprus.*

We are happy to follow the reviewer's suggestion to add data for the isoprene photoproduct mass. This is now done in Figure 5. However, it should be noted that this reflects only the emission of isoprene and photooxidation in the circa 10 km of land between to sea and the site. It does not give a representative regional perspective on the biogenic emission for Cyprus because of the short fetch of land between the coast and site (see answer to point 1).

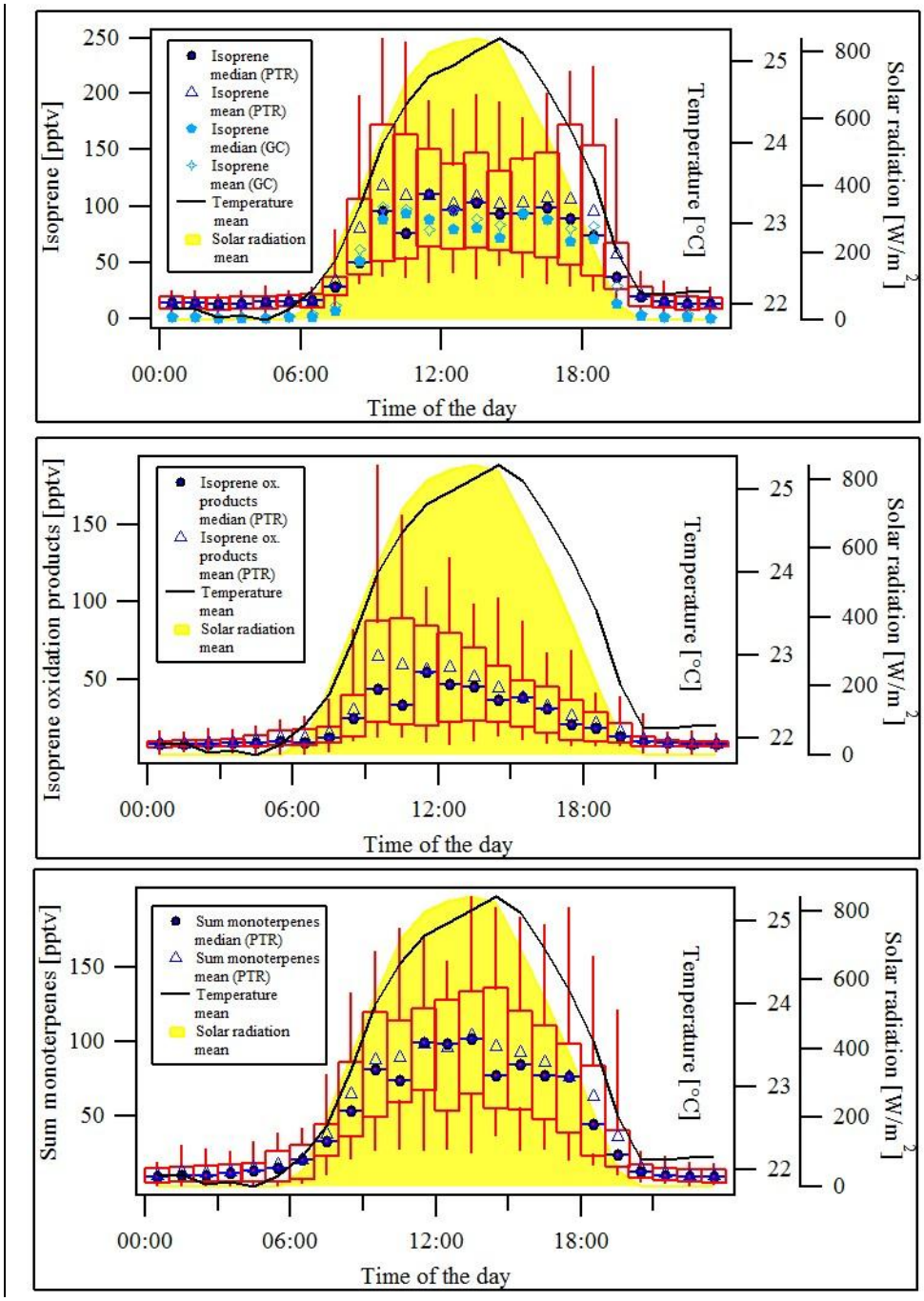


"Figure 5. Box and whiskers plots of isoprene, the oxidations products of isoprene and the sum of monoterpenes for the whole campaign with a 1 h time resolution as measured by the PTR-TOF-MS. For comparison the median and mean isoprene values measured by GC-MS were added in the upper panel. To calculate the boxplots PTR-TOF-MS data with a time resolution of 10 min and GC-MS data with a 45 min time resolution (20 min sampling time) were used. The contaminations in isoprene and the monoterpenes determined by comparing GC-MS and PTR-TOF-MS data were cut. The box contains 50% of the data. 25% of the data lie below the lower end of the box, 75% below the upper end. The whiskers present the 5–95% range of the data."

The following text was added:

"Another interesting tracer for the influence of biogenic emissions is the sum of the oxidation products of isoprene (methacrolein,methyl vinyl ketone and isoprene peroxidesmeasured atmass 71.0491 amu) which can be found in the midsection of Figure 5. The figure reveals that the level of the isoprene oxidation products, which is a function of the precursor isoprene mixing ratio and the OH concentration, was lower, but started to increase at the same time in the morning as the values of isoprene. MVK and MAC have a longer lifetime of 5-7 h with respect to OH ($2x10^6$ molec $cm^{-3}$) than isoprene. This means that these compounds can be transported over longer distances than isoprene. But the main wind direction was SW (see Fig.1), which means that the analyzed air masses were transported over the ocean for at least 12 h before reaching the site (see section 3.2.4). Furthermore the Mediterranean Sea is not a major source of isoprene. Therefore, transport of the oxidation products over long distances can be excluded. Still, the simultaneous increase of isoprene and its oxidation products means that the photochemical oxidation already took place. Most probably the majority of isoprene originates from the 10 km strip of land between the ocean and the site. During that short transport period oxidation already began. After midday OH decreases rapidly which leads to the decline in the mixing ratio of the oxidation products."

11. *Page 9 lines 280-295: discussion on Fig.5. How does RH change your results? How does RH impact the observations here? It is stated that "But as soon as the wind came from a region where the distance between ocean and site was shorter, isoprene levels decreased rapidly", which is awkward written and need to be improved by the way. However, from Fig.5., it seems the opposite. Isoprene level is clearly higher after _9:30AM than before it, so does DMS.*

As explained at length in response to point 5, great care has been taken in this dataset to account for changes in instrument sensitivity related to relative humidity. Each point is individually corrected for the humidity dependence and isoprene exhibited no humidity dependence for the reasons given previously. The intention in this section was to explain the morning peak in isoprene that occasionally occurred and which is exemplified in Figure 6. The text was changed as follows:

"Prior to the change in wind direction, the isoprene mixing ratio began increasing with temperature as expected. However, as soon as the local sea breeze set-in and the wind direction changed abruptly to the west, the isoprene levels decreased leaving an early morning spike. The apparent peak in isoprene at ca. 10:00 am is therefore generated by the wind change combined with the shorter section of isoprene emitting vegetated land between the site and the coast when the wind is from the west"

*12. Page 10 line 335-337: 'the measured production. . . the loss rate . . .' I don't think they are ever mentioned in the method part. Are they measured or calculated?*

The section containing these terms was completely revised and now the missing production rate for acetic acid at midday is calculated:

" To investigate this further the following formula was used to estimate the missing production rate for acetic acid around midday:

$$[Acid] = \frac{P_{res} + P_{OH}}{L_{OH} + L_{dep}}$$

$$P_{res} = [Acid] \times (L_{OH} + L_{dep}) - P_{OH}$$

where [Acid] refers to the mean acetic acid mixing ratio around midday, $P_{OH}$ to the photochemical production rate, $L_{OH}$ to the loss rate by the reaction with OH radicals, $L_{dep}$ to the dry deposition velocity. $P_{res}$ represents the residual production rate, which is the sum of several production terms such as emission from soil and vegetation as well as advection. The mean values at midday were determined from the diel cycles over the whole campaign. $L_{OH}$ was calculated by multiplying the mean value of OH around midday with its reaction rate constant with the acid, which gives a loss rate of 0.016 $h^{-1}$. The production rate $P_{OH}$ was calculated in the following way: average levels of acetaldehyde as the main precursor and of OH at midday and their reaction rate constant were multiplied, which gives the production rate of the acetyl peroxy radicals. Taking the measured concentrations of NO and $HO_2$ and their reaction rate constants with the acetyl peroxy radical into account it was found that the radical reacts to approximately 65% with NO and 35% with $HO_2$. It has been previously determined that 16% of the reaction between acetyl peroxy radical and $HO_2$ produce acetic acid (Groß et al., 2014). Thus, the production rate for acetic acid amounts to 0.0082 ppbv $h^{-1}$. This quite low production rate is consistent with the low level of PAA found. For the dry deposition velocity an area weighted average value of 0.427 cm/s was used, retrieved from the EMAC model. Ceilometer data from the site (height 650m above sea level) revealed an average of 250m for the PBL. Thus, the dry deposition velocity amounted to 0.061 ppbv $h^{-1}$. Applying these values leads to a remaining production rate of 0.087 ppbv $h^{-1}$. Due to the high uncertainty in many of the applied values the error of Pres amounts to ca. 133%."

*13. Page 11 Line 344-346: a) the authors state that secondary production is expected to be minor in a remote site due to a lack of precursors. However, this is only true if the sample is fresh. Are there any evidence suggesting the air is mostly fresh? Use some photochemical clocks could easily tell that (Isoprene/MVK+MACR, Benzene/Toluene, etc) b) I don't see evidence to support the conclusion that in-mixing from free troposphere contributed to the enhancement of acetic acid. It seems to be purely speculation here.*

a) As already described in point 12 this section was completely revised and now the missing production term is calculated.

b) The steep decrease in relative humidity and the parallel increase in ozone are a strong indication that the site was impacted by the residual layer/free troposphere. This is because ozone is rapidly deposited to surfaces in the boundary layer and the free troposphere is cooler and drier. Therefore we performed a new analysis, in which the periods affected by the residual layer/free troposphere are separated from the rest of the data set. A further graph showing the time traces of ozone and relative humidity is added to support this point (Fig. 10). Ozone mixing ratios are on average higher at night. This indicates that the site is in contact with the free troposphere. Otherwise the mixing ratios would decrease strongly during the night due to the high dry deposition rate for ozone and the low height of the nocturnal mixed layer. The nights during which the site was within the residual layer/free troposphere are marked in red.

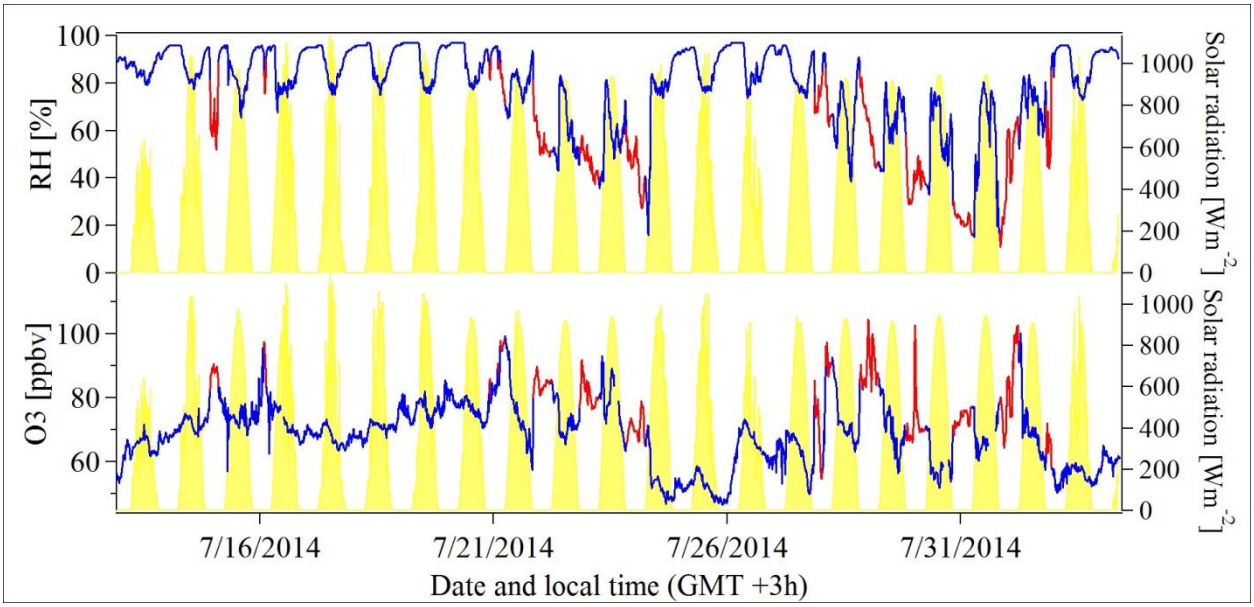


"Figure 10. Ozone in ppbv, relative humidty in % and solar radiation in $Wm^{-2}$ (10 min mean values). The red data points are influenced by air masses from the residual layer/free troposphere."

The following new analysis was added:

"During specific periods of the campaign, ozone showed higher values at night than during the day while relative humidity dropped drastically (see Figure 10). These features indicate that the site was within the residual layer/free troposphere (e.g. Fischer et al., 2003). To separate the

data the ozone values were multiplied by the mirrored relative humidity (100-RH). A threshold of 1000 ppbv % was chosen as a criterion of being in the residual layer/free troposphere. Furthermore, only night time periods were considered, because ceilometer data and vertical profiles from radio sondes confirmed that the site was within the boundary layer during the day. At night the mixed layer height calculations from the ceilometer data are unreliable, due to weak vertical mixing and the incomplete optical overlap of the lidar signal at low heights (Haeffelin et al., 2012). The time periods identified as being within the residual layer/free troposphere are color coded in red in Figure 10. Table 1 separates the averaged mixing ratios of different VOCs, O3 and CO, measured when sampling the residual layer/free troposphere and the PBL, additionally separated by east and west. It becomes clear that methanol, acetonitrile, acetone and acetic acid levels in the residual layer/free troposphere were higher than those measured in the PBL. Still, compared to the standard deviations, the differences are rather small, especially for acetone and acetic acid. When examining the data from the residual layer/free troposphere, a marked difference can be found between eastern and western flow regimes. Therefore it can be concluded that the source strength on the continents as well as the distance from the source to the site significantly influence the VOC levels."

"Table 1. Averaged data of VOCs, O3 and CO and their standard deviation in pptv based on a 10 min time resolution. The data were separated into periods reached by air from eastern or western regions as well as into values measured when the site was within the residual layer/free troposphere (RL/FT) and those recorded when the site was within the PBL."

| Compound | East RL/FT | Std. dev. east RL/FT | West RL/FT | Std. dev. west RL/FT | East PBL | Std. dev. east PBL | West PBL | Std. dev. west PBL |
|---|---|---|---|---|---|---|---|---|
| Methanol | 4389 | 866 | 3251 | 241 | 3328 | 841 | 2465 | 681 |
| Acetonitrile | 132 | 19 | 147 | 22 | 107 | 21 | 102 | 25 |
| Acetaldehyde | 345 | 112 | 190 | 33 | 377 | 153 | 254 | 95 |
| Acetone | 3158 | 694 | 2099 | 157 | 2531 | 463 | 1978 | 359 |
| Acetic acid | 1709 | 681 | 1039 | 165 | 1164 | 516 | 737 | 310 |
| Isoprene | 15 | 16 | 3 | 4 | 77 | 66 | 55 | 53 |
| Methylvinylketone Methacrolein/ISOPOOH | 9 | 7 | 4 | 3 | 31 | 30 | 23 | 31 |
| Methylethylketone | 124 | 40 | 44 | 10 | 128 | 30 | 87 | 16 |
| Benzene | 34 | 19 | 13 | 3 | 34 | 14 | 16 | 8 |
| Toluene | 5 | 3 | 2 | 2 | 11 | 8 | 6 | 5 |
| Total xylenes | 7 | 5 | 4 | 4 | 11 | 19 | 10 | 46 |
| Total trimethylbenzenes | 5 | 3 | 2 | 2 | 8 | 8 | 7 | 27 |
| Total monoterpenes | 11 | 14 | 4 | 2 | 66 | 57 | 46 | 42 |
| Ozone | 82364 | 9911 | 73096 | 5771 | 71463 | 7985 | 60090 | 7621 |
| Carbonmonoxide | 110522 | 11497 | 95484 | 7914 | 106593 | 10179 | 90715 | 6517 |

14. I am not convinced the usefulness of diel variability analysis for the whole campaign given there are clearly several meteorological/transport conditions during the period, while the paper still spend much effort to discuss the overall diurnal pattern, median vs mean values, etc. How about discuss those main transport conditions in more details?

As suggested by the reviewer we now expand Figure 7 (former Fig. 6) to include diel cycles from both the east and westerly flow regimes. Furthermore the periods where the site was withing the residual layer/free troposphere were excluded. The point we are making remains the same for acetone and methanol. There is no evidence of a consistently different diel cycle that could be related to different local emissions from the short strips of land between sea and site to the north and to the west. The measured mixing ratios of acetone and methanol are predominantly determined by emissions and subsequent photochemistry remote from the site. For the acetic acid data a clear diel cycle emerges which is analyzed in greater detail in section 3.2.1. For that reason acetic acid was now excluded from the analysis of the influence of the marine boundary layer transport in section 3.2.4.

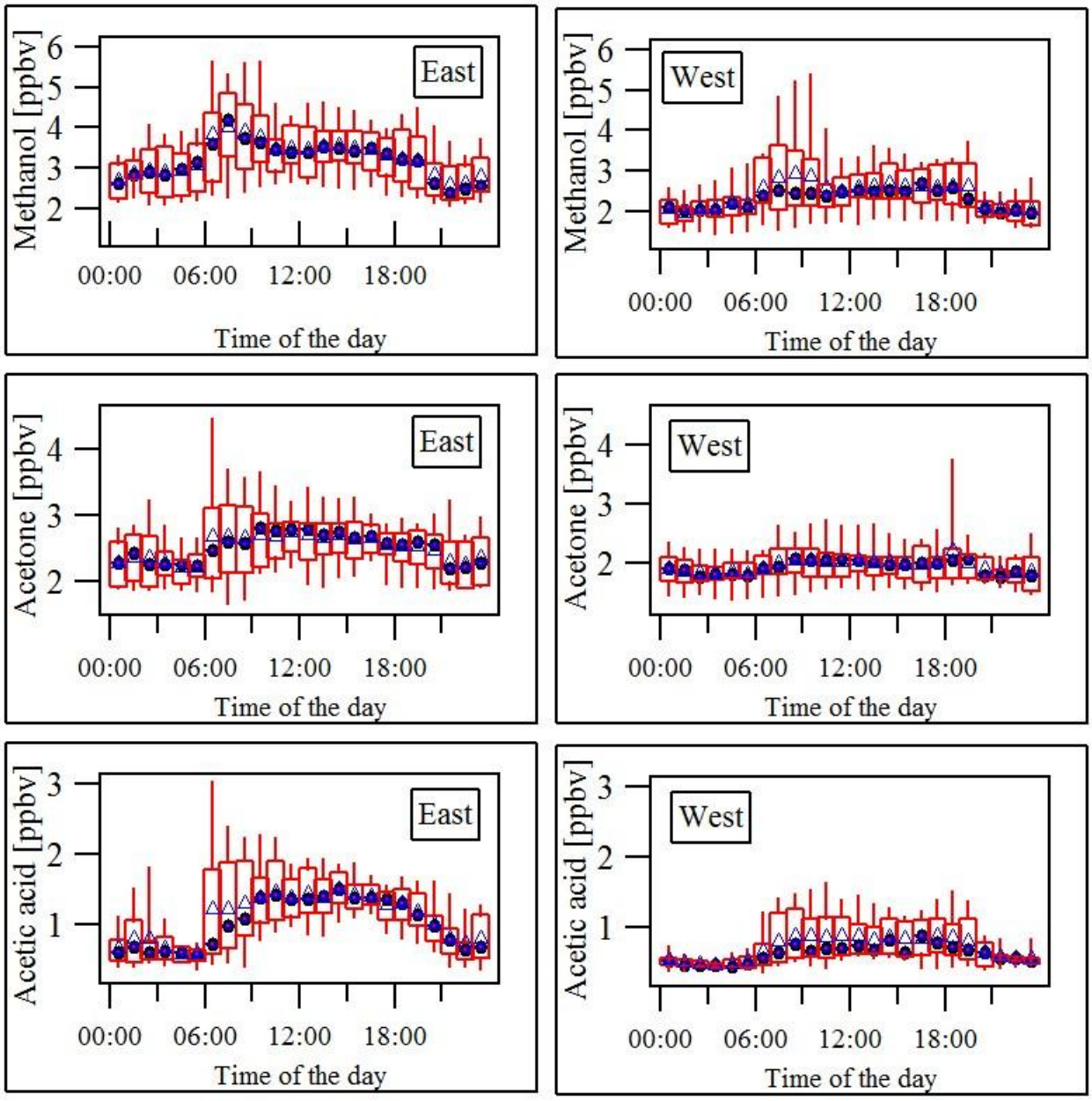


"Figure 7. Box and whiskers plot of acetone, methanol and acetic acid when the site was within the PBL. The triangles refer to mean and the circles to median values. The box contains 50% of the data. 25% of the data lie below the lower end of the box, 75% below the upper end. The whiskers present the 5–95% range of the data."

15. Ozone seems to be a good indication for fresh/aged air too. And the observed ozone is high. Are they coming from free troposphere, or are they from aged air? These could give insights on the VOC analysis particularly for acetic acid, but are lacking in the current version.

We take the reviewers point and refer them to our answer to 13b above. A further graph of the diel cycle of ozone and accompanying text has been added to support this point.

*16. Section 3.2.2: It is not clear how useful the box model is. Are the conclusions already well known? Given the boxing model is not constrained at the local scale, it seems to be not necessary to this paper.*

In this paper we attempt to determine the main processes causing variation in our measured species, particularly the OVOC species. In this context the box model provides valuable information as it can provide chemical mechanism based estimates of the rates of production and loss of our species during transport. We use the model to show that during transport methanol is lost while acetone is secondarily produced.

*17. Page 14, Line 447-451: a) Photolysis rate cannot be neglected for acetone given it is 1/3 -1/2 of its loss terms. B) How is OH measured? It is not mentioned in the method.*

a) The photolysis loss rate is small in comparison to the loss through OH and can be neglected in this assessment. The OH lifetime (assuming $2x10^6$ molecules $cm^{-3}$ OH) is circa 32days whereas the photolysis lifetime in the region, even in the upper troposphere where the photon flux is highest is between 75 and 250 days. Early budget estimations of acetone assumed a quantum yield of one, however, work by Blitz et al. (2004) and Arnold et al. (2005) have shown this to be wrong as the yield is temperature dependent. This considerably lengthens the photolysis lifetime.
   In order to clarify this assumption we insert the sentence, "Photolysis rates are so low that they can be neglected, in fact the ground level photolysis rate of acetone is at least ten times lower than the loss rate due to OH."

b) A full description of the OH instrument is now given in the method section. The inserted text is:
   "Atmospheric OH was recorded during Cyphex using the HORUS (HydrOxyl Radical measurement Unit based on fluorescence Spectroscopy) instrument based on the LIF-FAGE (Laser Induced Fluorescence-Fluorescence Assay by Gas Expansion) technique for atmospheric OH measurements. For further information please refer to (Novelli et al., 2014; Hens et al., 2014; Martinez et al., 2010).The precision for OH measurements is 4.8 x $10^5$ molec $cm^{-3}$ for 4 min time resolution. The accuracy for OH measurements is 28.5% (2s)."

*18. Page 14, line 459: a few place mentioned PBL height 500m. Is this a good assumption for this region?*

We believe that 500m is a good assumption for the marine boundary layer height in this study for the following reasons. Taking the definition of the boundary layer from Stull et al. (An

introduction to Boundary Layer Meteorology) we take the boundary layer as being "the part of the troposphere that is directly influenced by the Earth´s (or sea) surface, and responds to surface forcings on a timescale of an hour or less."
The following text was added:

"As already mentioned, ceilometer data from the site gave a PBL height of 250 m. This PBL was actually an internal boundary layer, that formed inside the marine boundary layer due to thermal and orographic effects, as it was advected over land. For the boundary layer over sea relevant to this study, an average PBL height of 500m was assumed. Previous aircraft studies in the region (Holzinger et al., 2005) focused on acetonitrile have reported vertical profiles over the sea that show sharp decreases in mixing ratios from 500m to 250m supporting the 500m boundary layer over sea assumption made here."

Previous regional studies have divided the atmosphere differently in the vertical dependent on the focus of the study. For example Lelieveld et al. (2002) considered the lower atmosphere including 0-4km and Traub et al. (2003) 0-2km (due to model resolution), although generally over continents values of 1-2 km are considered for the boundary layer height in high pressure regions (Stull). Marine boundary layer heights are generally lower and more stable because of the high heat capacity of water and correspondingly lower forcing changes. In the revised version we will support this boundary layer height assumption with the above text.

*19. Page 15, Line 484: again, the role of free troposphere should be clarified, and ozone could be helpful.*

See reply to point number 13.

*20. Page 15 Line 495: Ocean's role for OVOCs: Could correlations with DMS be more helpful?*

The reviewer is suggesting using DMS as a marker for ocean influence that can be used to elucidate the OVOC behaviour. Unfortunately, the process that produces marine DMS is different from the marine production and loss processes of the other OVOCs making this approach uncertain and complex. DMS is produced by certain marine microorganisms via enzymatic cleavage of DMSP, and as it is insoluble in water it is rapidly emitted to the air. Thus in productive regions there will be emissions and in oligotrophic regions not, and the location of these regions varies with time. The much more soluble acetone has been observed to be emitted by day and uptaken by night from seawater in productive waters, and when productivity decreases it can be uptaken all day. This is due to microbial consumption in the surface layer that creates a concentration gradient between air and water. Methanol is similarly consumed by microorganisms, however, significant photochemical production mechanism exists in the aqueous phase, particularly in productive waters. (Millet et al., 2008, Sinha et al., 2007, Dixon et al., 2014). Thus the correlation with DMS was not used.

*21. Section 3.2.4: I don't get too much information from this section. What is the main point? The lower CO emission for this region is interesting, but so do anthropogenic VOCs. An analysis based on transport pattern or aging would be more interesting.*

The purpose of this section is to provide correlation coefficients for the main species and variables studied here, for comparison with previous measurements (to observe regional emission changes e.g. lower CO emissions regional relative to 2003), for comparison with data from other regions by other practitioners, and for comparison with future studies in this region. Currently discussions are proceeding to create a large permanent measurement site on the west of Cyprus, so this CYPHEX dataset can provide an important first set of ratios with which future measurements can be compared. In the revised manuscript this section will however be made more concise.

## Referee 2

*1. Ln 71 Should add recent Muller et al paper (Nature Comm) to discussion of methanol budget.*

Thank you for this suggestion. The text was altered as described in point number 4.

*2. Ln 155. Would like more information on the large variation in the lab calibrations. Do the authors have any hypotheses for the challenges? Beyond adding uncertainty to the data, does the potential for RH dependent error alter any of the conclusions derived from these data?*

The following text was added:

"Literature confirms that the calibration of the PTR-TOF-MS for acetic acid represents a challenge: Warneke et al. (2001) found no humidity dependency, Feilberg et al. (2010) report a linear relation while Haase et al. (2012) state that the behavior strongly depends on the instrument itself. For the acid only one calibration was performed in the field with two different humidities. After the campaign a second calibration was done in the laboratory at three different humidities. In our case the calibration performed after the campaign is likely the more reliable, because the calibrations were performed at more humidity levels and using more calibration steps than in the field. Still, this calibration in the laboratory was done after the instrument was transported so that we cannot exclude that the sensitivity had changed. In the field as well as in the laboratory it was found that the sensitivity decreases with increasing humidity. The calibration factors obtained in the field and in the laboratory differed by a factor of ca. 2.5. Also the slope of the linear interpolations between the calibration factors of different humidities measured in the laboratory and in the field varied. Therefore the fit parameters of both linear regressions were averaged and the resulting mean fit function was used to calculate the calibration factor according to the humidity at the time. The discrepancy in the calibration

factors and problems during background measurement lead to a high total uncertainty of 51% and the detection limit amounts to 264 pptv."

*3. Please explain how the solubilities are determined for use in the models. For several compounds, these are pH sensitive (H*)?*

The reviewer has made essentially the same point as raised by Dr. Taraborrelli, namely that the H* values rather than Henry's Law constants should be used. The answer can be found below.

*4. Ln 270. This PP is confusing as earlier there is a discussion of what the ecology of the island is.*

We have amended the text to make this point more clear. The inserted text reads:

"The emission behavior of the monoterpenes indicates a domination of a light dependent emission regulation which is typical for vegetation without VOC reservoirs. Hence, coniferous tree species with resin ducts or herbal plants with glands play a minor role here. However, an emission classification of all the tree species found at the site is not available. Furthermore, we must take into account that VOC emissions from plant species with a temperature dependent release from storage pools may also show some degree of light dependency (Staudt et al., 1997; Owen et al., 2002)."

New references

Staudt, M., Bertin, N., Hansen, U., Seufert, G., Ciccioli, P., Foster, P., Frenzel, B., Fugit, J.L., (1997) Atmospheric Environment Vol. 31, No. SI, pp. 145-156.

Owen, S.M., Harley, P., Guenther, A., Hewitt, C.N. (2002) Light dependency of VOC emissions from selected Mediterranean plant species. Atmospheric Environment 36, 3147–3159.

## Comment by Dr. D. Taraborrelli

*The physical Henry's law coefficients (H) of methanol, acetone and acetic acid are used by the EMAC model and considered for the discussion of the results. However, for acetic acid the use of the effective coefficients (H*) is more appropriate. With an acidity constant (Ka) of 1.8E-5 M, an assumed mesophyll liquid pH of 7 and an ocean pH of 8.14, H* is estimated to be a factor of 181 and 2486 larger than H over vegetation and sea water, respectively. The authors might want to consider H* rather than H for acetic acid in their discussion.*

We thank D. Taraborrelli for his comment. He is completely correct that it is the effective Henry's law constant that needs to be considered in the calculation of dry deposition velocities, not the physical Henry's law constant.
Regarding our calculations with the EMAC model, several effective Henry's law constants have recently been updated (thanks again to D. Taraborrelli for pointing out some incorrect values in the previous code). The model runs described in the first version of the manuscript already used the corrected values. Our comparison with previous simulations with EMAC shows that acetic acid dry deposition velocity changes negligibly over the ocean surface upon using the correct H* value, which implies that the removal rate is limited by the aerodynamic and quasi-laminar boundary layer resistances and not the H*-inclusive surface resistance terms (see details in Kerkweg et al. (2006)).
However, in the revised version acetic acid is no longer used for the analysis in section 3.2.4. Furthermore the three different scenarios were cut in the revised paper and only a comparison between measurement and model is performed.
We have updated dry deposition velocities over the sea for methanol and acetone:

"The deposition velocities simulated in EMAC (Jöckel et al., 2016) over the Mediterranean Sea were taken and the area weighted average values amounted to 0.030 cm $s^{-1}$ for acetone and 1 x $10^{-4}$ cm $s^{-1}$ for methanol despite the higher solubility of methanol in comparison to acetone. The values are net deposition velocities calculated in a resistant-type scheme based on Wesely (1989) and implemented by Kerkweg et al. (2006), so they do not need to be proportional to the solubilities of the species."

New references:

Kerkweg, A., Buchholz, J., Ganzeveld, L., Pozzer, A., Tost, H., and Jöckel, P.: Technical Note: An implementation of the dry removal processes DRY DEPosition and SEDImentation in the Modular Earth Submodel System (MESSy), Atmos. Chem. Phys., 6, 4617–4632, doi: 10.5194/acp-6-4617-2006, 2006.

Wesely, M. L.: Parameterization of surface resistances to gaseous dry deposition in regional-scale numerical models, Atmos. Environ., 23, 1293–1304, 1989

In the following you can find the marked-up manuscript. Unfortunately changes in the graphs could not be highlighted, only the new graphs are implemented.
Here is a short overview over the changes made in the figures:

Fig. 2: Periods in which the CIMS measured PAA only or the sum of PAA and acetic acid are highlighted.

Fig. 3 (Fig. 5 in the revised version): Isoprene oxidation products measured by PTR-TOF-MS and isoprene data measured by GC-MS were added.

Fig. 4: Was split into 2 figures (now Fig. 3 and Fig. 4). These contain also GC-MS data for comparison.

Fig. 6 (now 7): The data for the calculation of the boxplots were separated into East and West. Furthermore data measured while the site was within the residual layer/free troposphere were excluded.

Fig. 8 (now 9): Acetic acid data were cut

Fig. 9 (now 11): Aceti acid data were cut

Fig. 10 and 11 can now be found in the supplement

Fig. 12 was cut

Fig. 13 (now 12): Shows an improved analysis (see revised section 3.2.4.)

Fig. 14, 15 and 16 were cut

New figures:

Fig. 10 shows time traces of ozone and relative humidity

Supplement S1: shows correlations between PTR-TOF-MS and GC-MS

Manuscript prepared for J. Name
with version 2014/09/16 7.15 Copernicus papers of the LaTeX class copernicus.cls.
Date: 29 April 2017

# Volatile organic compounds (VOCs) in photochemically aged air from the Eastern and Western Mediterranean

Bettina Derstroff[1], Imke Hüser[1], Efstratios Bourtsoukidis[1], John N. Crowley[1], Horst Fischer[1], Sergey Gromov[1], Hartwig Harder[1], Ruud H. H. Janssen[1,2], Jürgen Kesselmeier[3], Jos Lelieveld[1,4], Chinmay Mallik[1], Monica Martinez[1], Anna Novelli[1,5], Uwe Parchatka[1], Gavin J. Phillips[1,6], Rolf Sander[1], Carina Sauvage[1], Jan Schuladen[1], Christof Stönner[1], Laura Tomsche[1], and Jonathan Williams[1,4]

[1]Department of Atmospheric Chemistry, Max Planck Institute for Chemistry, Mainz, Germany
[2]Department of Civil and Environmental Engineering, Massachusetts Institute of Technology, Cambridge, Massachusetts, USA
[3]Department of Biogeochemistry, Max Planck Institute for Chemistry, Mainz, Germany
[4]Energy, Environment and Water Research Center, Cyprus Institute, Nicosia, Cyprus
[5]Institut für Energie- und Klimaforschung IEK-8: Troposphäre, Forschungszentrum Jülich GmbH, Jülich, Germany
[6]Department of Natural Sciences, University of Chester, Chester, United Kingdom

*Correspondence to:* Bettina Derstroff (bettina.derstroff@mpic.de), Jonathan Williams (jonathan.williams@mpic.de)

**Abstract.** During the summertime CYPHEX campaign (CYprus PHotochemical EXperiment 2014) in the Eastern Mediterranean, multiple volatile organic compounds (VOCs) were measured from a 650 m hilltop site in western Cyprus (34° 57' N / 32° 23' E). Periodic shifts in the northerly Etesian winds resulted in the site being alternately impacted by photochemically processed emissions from Western (Spain, France, Italy) and Eastern (Turkey, Greece) Europe. Furthermore, the site was situated within the residual layer/free troposphere during specific nights, which were characterized by high ozone and low relative humidity levels. In this study we examine the temporal variation of VOCs at the site. The sparse Mediterranean scrub vegetation generated diel cycles in the reactive biogenic hydrocarbon isoprene, from ~~below detection limit~~ very low values at night to ~~100~~80–100 pptv (1 pptv = $1 \times 10^{-12}$ mol mol$^{-1}$) by day on average. In contrast, the oxygenated volatile organic compounds (OVOCs) methanol and acetone exhibited ~~no diel cycle~~ weak diel cycles and were approximately an order of magnitude higher in mixing ratio (~~range:~~ ca. 2.5-3 ppbv by day on average, range: ca. 1–8 ppbv, 1 ppbv = $1 \times 10^{-9}$ mol mol$^{-1}$) than the locally emitted isoprene ~~(up to 320~~and aromatic compounds such as benzene (ca. 35 pptv ~~), total monoterpenes (up to 250~~by day on average, up to 130 pptv) and ~~aromatic compounds such as benzene and toluene (up to 100~~toluene (ca. 15 pptv ~~, spikes up to 400~~by day on average, up to 100 pptv). Acetic acid was present at mixing ratios between 0.05 and 4 ppbv ~~and~~ with ca. 1.2 ppbv during daytime on average. When data points directly affected by the residual layer/free troposphere were excluded, the acid followed a pronounced diel

cyclein one specific period, which was related to local influenced by various local effects including photochemical production and lossand local meteorological effects. During the rest of the campaign the impact of the free troposphere and long distance transport from source regions dominated over local processes and diel cycles were not observed, direct emission, dry deposition and scavenging from advecting air in fog banks. The Lagrangian model FLEXPART was used to determine transport patterns and photochemical processing times (between 12 hours and several days) of air masses originating from Eastern and Western Europe. Eastern and Western European air masses flow regimes showed distinct trace gas concentrations, with ca. 20 % higher ozone and ca. 30-5030-60 % higher values for most of the many OVOCs observed from the East. Using the FLEXPART calculated transport time, the contribution of photochemical processing, sea surface contact and dilution was estimated. Methanol , acetone and acetic acid all and acetone decreased with residence time in the marine boundary layer (MBL) with loss rates of 0.1 ± 0.01 ppbv/h, 0.06 rate constants of 0.031 ± 0.010.004 ppbv/h, 0.05 $h^{-1}$ and 0.022 ± 0.010.003 ppbv/h$h^{-1}$ from Eastern Europe and 0.06 ± 0.01 ppbv/h, 0.02 0.029 ± 0.0040.005 ppbv/hand 0.03 $h^{-1}$ and 0.014 ± 0.0040.003 ppbv/h$h^{-1}$ from Western Europe, respectively. The most soluble species, acetic acid, showed the lowest loss rates, indicating that solubility limited deposition to the ocean was not the only factor and that turbulent transport, plume dilution, microbial consumption within the surface of A theoretical calculation of the loss rate constants using the dry deposition velocities from the EMAC model revealed, that the ocean and especially entrainment from the free troposphere may also be importantcalculated results underestimate the measured values. The missing sink in the calculation is most probably an oceanic uptake enhanced by microbial consumption of methanol and acetone, although the temporal and spatial variability in the source strength on the continents might play a role as well. Correlations between acetone , methanol and acetic acid were rather weak and methanol were weaker in western air masses ($r^2$ =0.52–0.62 0.68), but were stronger in air masses measured after the shorter transport time from the East ($r^2$ =0.53–0.81 0.73).

Keywords: volatile organic compounds, Mediterranean, long distance transport, marine boundary layer, methanol, acetone, acetic acid, isoprene, monoterpenes

## 1 Introduction

The island of Cyprus is situated on the southeastern edge of the European Union. During the summer months, the east-west pressure gradient between the quasi-permanent South Asian monsoon low, the Persian trough and the Azores high induces northerly winds (Etesians), that overcome the westerly flow that is typical at temperate latitudes. The varying influences from the westerly and northerly winds make Cyprus an ideal vantage point to examine photochemically processed air from Eastern

and Western Europe. Despite a modest population (1.15 million in 2014 [1]) and little industrial emissions, the EU ozone air quality standard is regularly exceeded (Kourtidis et al., 2002; Kouvarakis et al., 2002; Gerasopoulos et al., 2005; Kalabokas et al., 2007, 2008, 2013; Doche et al., 2014; Kleanthous et al., 2014). The excess ozone is formed in sunlit conditions when volatile organic compounds (VOC), emitted from countries to the north and west of Cyprus, are oxidized in the gas phase by the atmosphere's primary oxidant, the OH radical in the presence of NOx ($NO + NO_2$) (Atkinson, 1990). In addition to ozone, numerous other secondary oxidants are formed including a suite of oxidized volatile organic compounds (OVOCs) such as alcohols (e.g. methanol), carbonyls (e.g. acetone), and organic acids (e.g. acetic acid). In this study we exploit the location and dual meteorological flow regime to investigate the abundance, temporal behavior, dependence on origin and the marine and tropospheric influence on VOCs. Several extensive studies of VOCs have been conducted previously in the Mediterranean area which have highlighted the relevance of anthropogenic, biogenic and biomass burning sources for regional chemistry. Airborne measurements have shown that the Mediterranean atmosphere is a ~~cross-road~~ cross roads for global pollution, with boundary layer chemistry driven by emissions from the European mainland, whereas the mid-troposphere (4–8 km) is influenced by North American emissions and above this, monsoon outflow from Asia (Lelieveld et al., 2002). Measurements made on Crete approximately one day downwind of mainland Greece revealed the enormous complexity of VOCs in the region (Xu et al., 2003). Moreover, it has been shown that the mixing ratios of many VOCs, especially OVOCs, in the Mediterranean strongly depend on long distance transport and are periodically influenced by biomass burning (Salisbury et al., 2003; Holzinger et al., 2005). Reactive biogenic species such as isoprene have also been shown to be emitted from Mediterranean vegetation (Kesselmeier et al., 1996; Liakakou et al., 2007).

Here we examine the relative impacts of biogenic emissions and long distance pollutant transport from Eastern and Western Europe on trace gas levels, with particular emphasis on VOCs. Moreover, we exploit the island location to investigate the influence of the sea on VOCs since air from Eastern and Western Europe was advected with variable transport times to the site within the marine boundary layer. The effect of the ocean on many VOCs, particularly OVOCs, can be significant and variable in latitude (Yang et al., 2013, 2014), biological activity (Taddei et al., 2009) and time of the day (Sinha et al., 2007).

To this end we have examined the behavior of an alcohol (methanol), a carbonyl (acetone), and an acid (acetic acid). Methanol is primarily emitted from plants (Galbally and Kirstine, 2002), with a relatively small photochemical production term in the estimated global budget, 37~~Tg~~ Tg $yr^{-1}$ from a total of 242 Tg $yr^{-1}$ found by Millet et al. (2008). However, recent model calculations by Müller et al. (2016) revealed that the photochemical reaction between methyl peroxy and hydroxyl radicals is, depending on the region, a significant source for methanol. The reaction was found to result in 115 Tg $yr^{-1}$ ~~(Millet et al., 2008)~~of methanol, which is in the range of the global terrestrial emissions.

[1] http://data.worldbank.org/country/cyprus; accessed on ~~4 May 2016~~22 April 2017

For example Millet et al. (2008) list a methanol source from terrestrial plant growth of 80 Tg $yr^{-1}$ and from plant decay of 23 Tg $yr^{-1}$. One of the main sinks of methanol is the oxidation by OH, while the role of the ocean is not completely characterized: Millet et al. (2008) report a methanol sink via OH oxidation of 88 Tg $yr^{-1}$ of a total sink of 242 Tg $yr^{-1}$. Furthermore Millet et al. (2008) state an oceanic source of 85 Tg $yr^{-1}$ and an ~~ocean uptake~~ oceanic sink of 101~~Tg $yr^{-1}$ of a total sink of 242 Tg~~ Tg $yr^{-1}$ which results in a net sink of 16 Tg $yr^{-1}$. ~~In contrast,~~ Jacob et al. (2005) found a loss of methanol via the reaction with OH of 129~~Tg $yr^{-1}$ while the ocean uptake amounts only to~~ Tg $yr^{-1}$ and an oceanic net sink of 10~~Tg~~ Tg $yr^{-1}$ from a total sink of 206~~Tg~~ Tg $yr^{-1}$.

According to Fischer et al. (2012) the global acetone budget sums up to 146~~Tg~~ Tg $yr^{-1}$, 32~~Tg~~ Tg $yr^{-1}$ being terrestrial emissions from biosphere and 31 Tg $yr^{-1}$ being photochemical production (26~~Tg $yr^{-1}$~~ Tg $yr^{-1}$ from isoalkanes, mainly anthropogenic, 5~~Tg~~ Tg $yr^{-1}$ biogenic). The main acetone sinks are photolysis and reaction with OH: Fischer et al. (2012) report a loss of 33~~Tg~~ Tg $yr^{-1}$ by OH oxidation and 19~~Tg~~ Tg $yr^{-1}$ by photolysis from a total sink of 146~~Tg~~ Tg $yr^{-1}$. Depending on the season and geographical location the ocean can either be a sink (82~~Tg~~ Tg $yr^{-1}$) or a source (80~~Tg~~ Tg $yr^{-1}$) of acetone ~~and is~~ (Fischer et al., 2012). Khan et al. (2015) on the other hand calculate a global acetone source of 72.7 Tg $yr^{-1}$, of which 55.6 Tg $yr^{-1}$ are photochemical production from $\alpha$-pinene, $\beta$-pinene and propane and 17.1 Tg $yr^{-1}$ direct emission. From the total sink of 72.9 Tg $yr^{-1}$ 30.8 Tg $yr^{-1}$ represent OH oxidation, 30.3 Tg $yr^{-1}$ photolysis and 11.8 Tg $yr^{-1}$ dry deposition and the ocean is regarded as being globally in a near equilibrium state ~~.~~(Khan et al., 2015). A global acetone source of 95 Tg $yr^{-1}$ was given by Jacob et al. (2002)~~on the other hand~~. The main contributions are emissions by terrestrial vegetation (33 Tg $yr^{-1}$), by the ocean (27 Tg $yr^{-1}$) and the oxidation of isoalkanes (21 Tg $yr^{-1}$). Jacob et al. (2002) determined a sink by OH reaction of 27~~Tg~~ Tg $yr^{-1}$ and by photolysis of 46~~Tg~~ Tg $yr^{-1}$ from a total loss of 95~~Tg~~ Tg $yr^{-1}$.

Most of the acetic acid budget is in-situ photochemical production, about 59~~Tg~~ Tg $yr^{-1}$ from a total source of 86~~Tg~~ Tg $yr^{-1}$. The total acetic acid sink of 86~~Tg~~ Tg $yr^{-1}$ consists of approximately 1/3 photochemical loss (25~~Tg~~ Tg $yr^{-1}$), 1/3 wet deposition (27~~Tg~~ Tg $yr^{-1}$) and 1/3 dry deposition (31~~Tg~~ Tg $yr^{-1}$) (Paulot et al., 2011).

Using the rate coefficient ~~(k)~~ for each OVOC provided by IUPAC (Atkinson et al., 2006) and the diel mean OH concentration of $2 \times 10^6$ molec $cm^{-3}$ measured during the campaign, the following atmospheric lifetimes with respect to the removal by OH were calculated: 6 days for methanol, 32 days for acetone and 8 days for acetic acid.

This study was designed to investigate the chemical characteristics of polluted air emerging from the European continent which is then photochemically processed over the Mediterranean Sea between 12 hours and several days en-route to the island of Cyprus. It is therefore in contrast with most atmospheric chemistry campaigns that generally investigate source impacted locations (e.g. in forests and megacities). The novelty of the CYPHEX (CYprus PHotochemical EXperiment) campaign for VOC research was ~~threefold~~fourfold: firstly, the relative local impacts on biogenic and transported

VOCs were assessed; secondly, Eastern and Western European outflow was chemically characterized and contrasted ; ~~secondly, the relative local impacts on biogenic and transported VOCs were assessed and thirdly~~thirdly, the impact of air masses originating from the residual layer/free troposphere was examined and fourthly, the influence of summertime Mediterranean marine boundary layer transport on OVOCs was investigated.

~

## 2 Experimental

### 2.1 Site

The measurement site (Ineia) is situated on the northwest coast of Cyprus at the top of a 650 m hill located ca. 10 km from the shoreline (34°57' N / 32°23' E). The surrounding area (5 km radius) is rural in character, comprising of farmland and a few small villages (e.g Ineia population 367 [2]). Extending 25 km to the northwest was the Akamas peninsula national park and to the northeast the terrain descended rapidly to the city of Polis (population 1975 [3]) at sea level. Although Cyprus has a population of over 1 million their emissions do not influence this dataset since no Cypriot cities or industries lie upwind of the site. Instead the measurements analyzed here represent the transported and photochemically processed pollution emerging from Eastern and Western Europe. The vegetation is sparse and scrub like. Small trees such as the native pine (*Pinus brutia*), juniper (*Juniperus phoenicea*) and olives (*Olea europea*), Carob (*Ceratonea siliqua*) are interspersed amidst low lying bushes such as *Inula viscosa* and *Foeniculum vulgare*. In addition small groves of vines, almonds and pomegranates are kept by some local farmers. In summer, Cyprus is normally influenced by the Etesian winds, which bring air masses from the north (from Eastern Europe, and crossing Turkey and Greece). However, in 2014 a southward displacement of the storm track and associated synoptic weather systems weakened the east-west pressure gradient (Tyrlis et al., 2015) delaying the onset of the Etesian winds and causing periodic influence of air advected from the West over the Mediterranean Sea. Despite clear variation in air mass origin during this campaign (12 July–03 August 2014) the local wind direction at the site was primarily SW (~~72~~ca. 70 %, see Fig. 1).

### 2.2 Instrumentation

Measurement instruments were installed in four air-conditioned laboratory containers, positioned in two stacks of two with a 8 m tall, 0.5 m diameter, high flow (10 $m^3$ $min^{-1}$) common inlet situated between the stacks (see Fig.1). The common inlet was designed to minimize wall losses of species in air drawn from the 8 m high sampling point, and to avoid small scale measurement differences caused by individual inlet positioning. For the measurement of VOCs a slower subsample flow (5 L $min^{-1}$)

[2] http://www.populationlist.com/~~Eparchia_Pafou/06/760931/state-population~~; accessed on ~~16 August 2016~~22 April 2017

[3] http://www.populationlist.com; accessed on 22 April 2017

was drawn through insulated and heated (ca. 35 °C) Teflon lines (OD = 1.27 cm) installed perpendicular to the direction of main inlet flow and into the VOC group measurement container. This air was analyzed by a Proton Transfer Reaction Time Of Flight Mass Spectrometer (PTR-TOF-MS), an OH reactivity system, two Gas Chromatography systems with a Flame Ionization Detector (GC-FID) and one Gas Chromatography system combined with a Mass Spectrometer (GC-MS).

### 2.2.1 Proton Transfer Reaction Time of Flight Mass Spectrometer

On-line VOC measurements were performed with a PTR-TOF-MS (Ionicon Analytik GmbH, Innsbruck, Austria). This instrument has been described in detail elsewhere (Graus et al., 2010; Veres et al., 2013). Post-acquisition data analysis was performed using the program "PTR-TOF DATA ANALYZER", which is detailed elsewhere (Müller et al., 2013). The time resolution of the measurements was 1 min~~and the background level~~ , but for the data analysis in this publication 10 min average values were used. The background signal was determined every two hours for twenty minutes by passing air through a catalytic converter containing platinum coated pellets heated to 320 °C. The drift pressure was maintained at 2.20 mbar and the drift voltage 600 V (E/N 137 Td). To perform mass scale calibration 1,3,5-trichlorobenzene was permanently bled into the sample stream as an internal standard.~~A~~

At the beginning and at the end of the campaign a comprehensive 4 point ~~humidity dependent~~ calibration of the instrument (spanning the measured range of compounds) was performed at 4 and 3 different humidities, respectively. The humidity level was determined by using the ratio between the isotope of the water cluster and the ~~beginning and at the end of the campaign using a~~ isotope of the primary ion and this ratio lay between 0.07 and 0.3 for the different calibrations. These values correspond approximately to a range of 25 % to 80 % relative humidity. A commercial gas standard (Apel-Riemer Environmental) containing 14 compounds was used. Great care was taken to account for this humidity dependence in each datapoint. The sensitivity of the instrument ~~, which was interpolated linearly over the campaign and is expressed in normalized counts per second per ppbv (ncps ppbv$^{-1}$) , decreased by a range of 0.6~~for each individual data point was derived from a linear interpolation over time between the two calibrations and corrected for the co-measured ambient relative humidity at that time. The decrease in sensitivity between the two calibrations (2.5 weeks apart) were generally modest, ranging from 10 ~~ncps ppbv$^{-1}$~~ % (e.g. isoprene) to ~~3~~23 ~~ncps ppbv$^{-1}$~~ % (e.g. methanol).

~~With~~ Most compounds measured by PTR-TOF-MS show a more pronounced humidity dependence between 0 and ca. 15 % relative humidity (whereby dry conditions are most sensitive), but with increasing humidity the ~~sensitivity decreased exponentially for most of the species. Only~~ dependency weakens so that decreases in sensitivity in the upper humidity range are very small. This behavior which was described by an exponential fit function was observed for all compounds except isoprene and methanol. Isoprene shows almost no humidity dependency, because its reaction rates with

the primary ion and the water cluster have roughly the same value as has been previously reported by Smith et al. (2001). The variations in the sensitivity for methanol did not show ~~any humidity dependency.~~ the same characteristic exponential behavior described above, so that no interpolation was made. However, since the values showed a variation of only 5-10 %, an averaged calibration factor was used instead. The underlying reason for this anomalous behavior is not known in the case of methanol.

Calibration factors were applied by taking the time of the measurement as well as the humidity for each data point into account. Detection limits for each species quantified were determined by calculating ~~three times~~ the standard deviation of ~~the~~ each background measurement. The highest value of these standard deviations was multiplied by 3 to give the detection limit (3 $\sigma$, 1 minute time resolution). The results lay between ~~15~~8 pptv (e.g. ~~acetonitrile) and 200~~monoterpenes) and 242 pptv (methanol). 1 pptv is defined as $1 \times 10^{-12}$ mol mol$^{-1}$. The total uncertainty is defined by the statistical error, which was calculated from the ~~geometric combination of the~~ noise, and the systematic error. The latter contains the error of the calibration, the flow measurements, the calibration gas bottle accuracy as well as the maximum error occurring due to changes in sensitivity. For acetaldehyde an extra term was added that takes problems during background measurements into account. During a few periods of the campaign the ambient humidity was below the lower limit of the calibrated humidity range. The absence of a trend for methanol and isoprene precluded interpolation, while the exponential fit for the other compounds is afflicted with a higher error in this range. The variation in sensitivity in the range below 25 % relative humidity was estimated from previous measurements in our laboratory and was included in the error calculation. The values of the total uncertainty within the calibrated range varied between 10~~and 15~~ % (e.g. isoprene) and 23 % ~~. Only methanolhad a higher total uncertainty of 30~~(e.g. methanol) and increased to a maximum of 28 % ~~due to problems during calibration.~~ (methanol) in the low humidity range.

Acetic acid was calibrated separately by the use of a permeation source, because it was not included in the pressurized gas standard. Literature confirms that the calibration of the PTR-TOF-MS for acetic acid represents a challenge: Warneke et al. (2001) found no humidity dependency, Feilberg et al. (2010) report a linear relation while Haase et al. (2012) state that the behavior strongly depends on the instrument itself. For the acid only one calibration was performed in the field with two different humidities. ~~As found by Feilberg et al. (2012) the humidity dependency of acetic acid shows a linear behavior.~~ After the campaign a second calibration was done in the laboratory at three different humidities. In our case the calibration performed after the campaign is likely the more reliable, because the calibrations were performed at more humidity levels and using more calibration steps than in the field. Still, this calibration in the laboratory was done after the instrument was transported so that we cannot exclude that the sensitivity had changed. In the field as well as in the laboratory it was found that the sensitivity decreases with increasing humidity. The calibration factors obtained in the field and in the laboratory differed by a factor of ca. 2.5. Also the slope of the linear interpo-

lations between the calibration factors of different humidities measured in the laboratory and in the field varied. Therefore the fit parameters of both linear regressions were averaged and the resulting mean fit function was used to calculate the calibration factor according to the humidity at the time. The discrepancy in the calibration factors ~~leads~~ and problems during background measurement lead to a high total uncertainty of ~~47%~~ 51% and the detection limit amounts to 264 pptv.

Acetic acid was measured at mass 61.0284 amu, but its mixing ratios must be considered as upper limits, because the PTR-TOF-MS is not able to distinguish between acetic acid and its isomer glycolaldehyde (Baasandorj et al., 2014). Furthermore, fragments of peroxyacetic acid (PAA) and ethyl acetate can also be measured on the exact mass of acetic acid (Baasandorj et al., 2014). However, since the sources of ethyl acetate are mainly anthropogenic and the measurement site remote, we assume that the influence of ethyl acetate was negligible. This assumption is supported by the finding that the signal at 61.0284 amu was significantly reduced during periods when the site was impacted by fog, indicating that the responsible trace gas was highly soluble in water. The potentially interfering molecule ethyl acetate is not nearly as soluble: 0.059 mol $m^{-3}$ $Pa^{-1}$ in comparison to 40-46 mol $m^{-3}$ $Pa^{-1}$ for acetic acid, see (Sander, 2015).

The PTR-TOF-MS was not calibrated for PAA and ~~monitored it only during a few days of the campaign at mass 77.0233 amu. On these days the PAA signal in counts per second (cps) was very low~~ only detected it with low count rates (ca. 0.3 cps) at mass 77.0233 amu for a few days of the campaign. Španěl et al. (2003) reported that 90 % of ~~PAA are~~ protonated PAA is measured at the exact mass of acetic acid, while 10 % are recorded at the mass of the mother ion (77.0233 amu). If this is taken into account, PAA would still influence acetic acid~~only between~~ , but between only ca. 10 and ~~20~~15 % because of the low count rates.

A Chemical Ionization Mass Spectrometer (CIMS) designed to measure PAA was operated in two modes during the campaign (Phillips et al., 2013). From $\sim$ 17–24 July the CIMS measured PAA only and found very low values, close to the detection limit. From $\sim$ 26 July until the end of the campaign the collisional dissociation parameters were adjusted and PAA and acetic acid were detected on the same mass (59 amu). It was only discovered after Cyphex that the CIMS measured not only PAA but also acetic acid, and the approximate, relative sensitivity to PAA and acetic acid was only determined a year later. For this reason, the absolute values for the CIMS data are highly uncertain, but ~~reveal~~ indicate that PAA levels were substantially lower than those of acetic acid. Figure 2 displays the acetic acid and the PAA traces as well as their correlation and it can be seen that the PAA data without accompanying detection of acetic acid (~~blue~~ black line) showed very low values between 0 and 200 pptv from $\sim$ 17–24 July. The later period from $\sim$ 26 July until 3 August exhibited much higher signals due to the sum of PAA and acetic acid (red line). The correlation in the CIMS and the PTR-TOF-MS time profiles for the later period with a correlation factor of 0.74 suggests that most of this is due to acetic acid. ~~The~~ A direct comparison between the absolute acetic acid values measured by the CIMS and the PTR-TOF-MS system is not possible, because the CIMS signal was analyzed

as PAA. Still, due to the very low PAA levels it can be concluded that the potential interference in the PTR-TOF-MS signal for acetic acid is ~~thus~~ small compared to the ~~47~~51% total uncertainty of the acetic acid measurements.

The main sources of glycolaldehyde, which is an isomer of acetic acid and can therefore not be ~~distiguished~~ distinguished from the acetic acid signal, are biomass burning and secondary production from isoprene and ethene degradation (Niki et al., 1981; Paulson and Seinfeld, 1992). Since the acetonitrile levels stayed low during the whole campaign we can exclude a significant influence of biomass burning. Furthermore, as will be shown in the results section, isoprene levels were low due to the scarce vegetation and low local anthropogenic emissions occurred. The atmospheric lifetime of glycolaldehyde was calculated taking the removal by OH and photolysis into account. During the campaign an average OH concentration of $\sim 2 \times 10^6$ molec cm$^{-3}$ and an average photolysis rate of $\sim 3 \times 10^{-6}$ s$^{-1}$ were determined. Using a reaction rate of $8.0 \times 10^{-12}$ cm$^3$ molec$^{-1}$ s$^{-1}$ provided by IUPAC (Atkinson et al., 2006) a lifetime of ~15 h was calculated. Wet and dry deposition were not considered in this calculation and would reduce the lifetime even further. In most cases the air masses measured remained roughly 12 h to 5 days over the Mediterranean Sea before reaching Cyprus. This would mean that some glycolaldehyde could survive transport, especially during night, but the amount is expected to be small. Since there is no known ocean source for glycolaldehyde, we can assume that this compound has only a minor effect on the acetic acid signal.~~In view of the discussion above , the acetic acid mixing ratios shown in the following analysis may be regarded as an upper limit~~

For the reason stated above the remainder of this paper treats mass signals 33.0335 amu, 59.0491 amu and 61.0284 amu as methanol, acetone and acetic acid, respectively.

~

#### 2.2.2 Monoterpenes, ozone, CO, OH and meteorological parameters

~~Monoterpenes were measured~~ Isoprene and monoterpenes ($\alpha$-pinene, $\beta$-pinene , $\Delta$-3 carene and limonene) were also quantified by a commercial GC-MS system (MSD 5973; Agilent Technologies GmbH) combined with an air sampler and a thermal ~~desorber~~ desorption unit (Markes International GmbH)~~and the~~ . The sample interval was 45 min, the sampling time amounted to 20 min, while calibrations were carried out every 8-12 samples with a commercial gas standard mixture (National Physical Laboratory, UK). The detection limit was 1 - 2 pptv and the total uncertainty ca. 15 %. The volatiles were trapped at 30 °C on a low-dead-volume quartz cold trap (U-T15ATA; Markes International GmbH), which was packed with two sorbent beds (Tenax TA and Carbograph I). The trap was then heated to 320 °C and the compounds were transferred to a 30 m GC column (DB-624, 0.25mm I.D., 1.4$\mu$ m film; J&W Scientific). The temperature of the GC oven was programmed to stay stable at 40 °C for 5 min, thereafter increase to 140 °C with a rate of 5 °C/min and finally the rate was increased to 40 °C/min to reach the final temperature of 230 °C, which was held for 3 min.

Due to co-elution of $\beta$-pinene and $\Delta$-3 carene, a separation was not possible and therefore the signal was treated as the sum of the two species.

Ozone was monitored using a U.V. Photometric $O_3$-Analyzer (model 49, Thermo Environmental Instruments, U.S.) The detection limit was 2 ppbv ((1 ppbv = $1 \times 10^{-9}$ mol mol$^{-1}$) and the overall uncertainty less than 5 %.

CO was measured by a Room Temperature Quantum Cascade Laser (RT-QCL) (Li et al., 2012). The instrument uses wavelength modulation absorption spectroscopy (2190 cm$^{-1}$) over a path length of 36 m to measure CO at a time resolution of 1 s. The detection limit was determined to be 0.4 ppbv and the overall uncertainty 14.4 %. ~~For more~~

Atmospheric OH was recorded during Cyphex using the HORUS (HydrOxyl Radical measurement Unit based on fluorescence Spectroscopy) instrument based on the LIF-FAGE (Laser Induced Fluorescence-Fluorescence Assay by Gas Expansion) technique for atmospheric OH measurements. For further information please refer to ~~Li et al. (2012~~(Novelli et al., 2014; Hens et al., 2014; Martinez et al., 2010). The precision for OH measurements is $4.8 \times 10^5$ molec cm$^{-3}$ for 4 min time resolution. The accuracy for OH measurements is 28.5 % ($2\sigma$).

The weather station Vantage Pro2 (Davis Instruments Corp., Hayward, CA) was used to measure temperature, pressure, wind direction and speed, solar radiation and humidity with a time resolution of 1 minute.

A Jenoptik CHM15k ceilometer was used to observe the aerosol backscatter profile, and the STRAT-2D algorithm (Haeffelin et al., 2012) to calculate the mixed-layer height from this observed aerosol backscatter profile.

## 2.3 Modeling

### 2.3.1 FLEXPART model

The dynamical transport history of air reaching Cyprus during the CYPHEX campaign was determined by using the Lagrangian particle dispersion model FLEXPART (Stohl et al., 2002, 2005, 2007). It computes trajectories of infinitesimally small air parcels (so-called particles) to describe the transport and diffusion of tracers (Stohl et al., 2005). Thereby mean winds interpolated from analysis fields and turbulence represented by random motions are used (Stohl et al., 2007).

In this study, FLEXPART was run backward in time from the measurement site driven with analyses from the ECMWF with $0.2^\circ \times 0.2^\circ$ horizontal resolution (derived from T799 spectral truncation), a vertical resolution of 137 model levels and temporal resolution of 1 h, which was a combination of 6 h analyses and short-term forecasts. Backward simulations were made for 3 h time intervals between 12 July 2014 and 03 August 2014 and for each interval 10000 passive air tracer particles were released and followed backward in time for 120 h. The distribution of tracer particles was analyzed during the 120 h simulation and led to a particle density distribution describing the residence time

in each cell of a defined geographical grid. Column-time integration of residence times resulted in a horizontal distribution indicating the total upwind area of influence. Regions of higher residence times during the simulation period identified major transport routes of air reaching the site.

#### 2.3.2 CAABA/MECCA

To investigate photochemical processing over the ocean, the observations were compared to simulations with the chemical box model CAABA/MECCA (Sander et al., 2011). We used version 3.8, which includes the recently developed comprehensive organic reaction scheme MOM (Mainz Organics Mechanism) by Lelieveld et al. (2016). Focusing on organics, we switched off halogen and sulfur chemistry, as well as heterogeneous and aqueous phase reactions in view of the low cloudiness and aerosol concentrations. Initial values based on the EMAC model (Jöckel et al., 2016) are available in the supplement together with a complete list of chemical reactions used in this study, rate coefficients and references. Photolysis rate constants were calculated for the latitude of Cyprus. The model simulated a period of two days, starting on 19 July at 6 am. No further emissions were injected during the model run, except ozone to simulate its entrainment from the residual layer/free troposphere into the boundary layer. Dry deposition as well as uptake by aerosols were not considered in this study. The results will be discussed in section 3.2.3.

## 3 Results

### 3.1 Biogenic compounds

In general, the mixing ratios of biogenic compounds measured at the site were low, with the sum of isoprene (m/z 69.0699 amu) and monoterpenes (m/z 137.1325 amu) never exceeding ~~0.5~~500 ~~ppbv~~ pptv and a campaign average daily maximum of ~~0.1~~100 ~~ppbv for both~~pptv for both, measured by the PTR-TOF-MS. This is in contrast to tropical forest regions where typical values of ~~8~~7.6 ppbv isoprene and 1 ppbv monoterpene have been reported recently (Yañez Serrano et al., 2015) ~~, but~~ and boreal forest regions where levels of isoprene and monoterpenes are ca. 100 pptv and 300 pptv respectively (Yassaa et al., 2012). The measured values in this study are consistent with levels reported previously from the Mediterranean areas (Liakakou et al., 2007; Davison et al., 2009). Comparable emission rates of isoprene and the sum of monoterpenes can be regarded as typical for the Mediterranean vegetation (Kesselmeier and Staudt, 1999). Isoprene and several different monoterpenes were also measured by a GC-MS system operating at a lower time resolution at the same site. A comparison between the results of the two instruments can be found in the Figures 3 and 4. PTR-TOF-MS data with a 1 min time resolution were merged onto the 20 min sampling time of the GC-MS. The dashed line in these figures refers to a time period where a contamination in the PTR-TOF-MS is assumed. This period was excluded from the comparison. During the day the isoprene data measured by the PTR-TOF-MS were ca. 1.3 times higher than the GC-MS data

(Figure 3), while at the low level nighttime values the PTR-TOF-MS system measured ca. 7.5 times more isoprene than the GC-MS (determined from diel median values over the whole campaign). An insufficient determination of the humidity dependency of the PTR-TOF-MS for isoprene can be ruled out as a possible explanation, because isoprene measurements are not dependent on humidity (see section 2.2.1). A correlation of the two datasets (PTR vs. GC data) using a bivariate fit algorithm resulted in a slope of 1.2, an intercept of 10.4 pptv and a $r^2$ value of 0.88. The reason for the discrepancy is yet unknown. The correlation plots between PTR-TOF-MS and GC-MS measurements can be found in the supplement S1. The data were color coded by the date and time of the recording. It becomes clear that the agreement between the two data sets varied slightly with time. Thus, an instrumental issue during a specific period can not be ruled out. The lower part of Figure 4 shows the data of $\alpha$-pinene, the sum of $\beta$-pinene and $\Delta$3-carene as well as limonene measured by the GC-MS system. The sum of the monoterpenes measured by GC-MS are compared to the total monoterpene signal measured by PTR-TOF-MS at 137.13 amu in the upper part. The PTR-TOF-MS data are up to 2.5 times higher than the GC data (determined from diel median values over the whole campaign). This can partly be explained by the fact that the sum on mass 137 amu can also contain monoterpenes other than those quantified by the GC-MS. The correlation between the two signals (bivariate fit algorithm, PTR vs. GC) lead to a slope of 1.6, an intercept of 0.64 pptv and a correlation coefficient $r^2 = 0.80$. This is reasonable given unmeasured monoterpenes by GC-MS. Furthermore, the total monoterpene signal of the PTR-TOF-MS system was calibrated with $\alpha$-pinene. Thus, slight differences in sensitivity, which occur as soon as $\alpha$-pinene is not the dominant species, can play a role.

Since both isoprene and monoterpenes have atmospheric lifetimes on the order of minutes to hours with respect to the removal by OH, we concluded that they must have been emitted by local vegetation. Based on ceilometer measurements, they are emitted into a shallow boundary layer of maximum 250 m. Figure 5 displays the campaign 1h - averaged, diel cycles of the sum of the monoterpenes and of isoprene ~~. Both~~ measured by the PTR-TOF-MS instrument. For comparison the GC-MS data of isoprene were added in the upper panel. Keeping in mind that the low time resolution of the GC-MS might statistically bias the result, both instruments show a reasonably similar profile. The median diel cycles of isoprene and the monoterpenes follow a roughly sinusoidal curve and were strongly light dependent. This finding is consistent with the literature concerning isoprene and monoterpene emissions and atmospheric mixing ratios in the Mediterranean area (Kesselmeier et al., 1998; Liakakou et al., 2007; Davison et al., 2009).

~~Figure ?? shows the course of isoprene and the main monoterpene species as observed over the whole campaign detected by a~~ Due to the light dependent profiles, it was expected that isoprene levels would decrease to nearly zero at night, which is the case for the GC-MS ~~system with $\alpha$-pinene being the dominant species among the monoterpenes quantified. At night the values were close to the detection limit of the PTR-TOF-MS, but the GC-MS data revealed that the mixing ratios of~~

isoprene and monoterpenes decreased to nearly zero in almost all nights (see Figure ??). This light dependent signal, but not for the data measured by PTR-TOF-MS. Therefore it can be concluded that the GC-MS system provides more reliable absolute values. But, since the focus shall now be placed on the course of the profile and not on the absolute levels, the PTR-TOF-MS data are used in view of the higher time resolution. The emission behavior of the monoterpenes indicates that the vegetation is dominated by broad leaf species . Conifers, on the other hand, are able to store specific monoterpenes and emit them also depending only on temperature or other stress (Kesselmeier and Staudt, 1999, and references therein) so that elevated levels could also be found at night (e.g. Davison et al., 2009; Staudt et al., 1997)a domination of a light dependent emission regulation which is typical for vegetation without VOC reservoirs. Hence, coniferous tree species with resin ducts or herbal plants with glands play a minor role here. However, an emission classification of all the tree species found at the site is not available. Furthermore, we must take into account that VOC emissions from plant species with a temperature dependent release from storage pools may also show some degree of light dependency (Staudt et al., 1997; Owen et al., 2002).

The mean isoprene mixing ratios (Fig. 5) show slightly elevated values in comparison to the median values in the morning and afternoon. A potential explanation can be found by considering the changes in meteorological conditions during these parts of the day, e.g. variation of the local boundary layer height relative to the hilltop site or the onset of the local sea breeze. The impact of these changes varied during the campaign, potentially causing the difference between median and mean valuesand motivates a closer look to single days. To exemplify this, isoprene from 22 July has been plotted at 1 minute time resolution (Fig. 6). On that day at around 9:30 am local time the wind changed from N-NE to W-SW direction as which was accompanied by a sharp increase in relative humidity and in atmospheric dimethylsulfide (DMS), a species primarily emitted from marine sources (Cline and Bates, 1983; Mesarchaki et al., 2014). Before the wind direction changed, isoprene initially increased together with temperature . But Prior to the change in wind direction, the isoprene mixing ratio began increasing with temperature as expected. However, as soon as the wind came from a region where the distance between ocean and site was shorter, local sea breeze set-in and the wind direction changed abruptly to the west, the isoprene levels decreased rapidlyleaving an early morning spike. The apparent peak in isoprene at ca. 10:00 am is therefore generated by the wind change combined with the shorter section of isoprene emitting vegetated land between the site and the coast when the wind is from the west. This behavior is consistent with the current understanding that the sea is only a weak source of isoprene and the main source is the local terrestrial vegetation (Bonsang et al., 1992; Broadgate et al., 1997; Palmer and Shaw, 2005; Arnold et al., 2009). However, isoprene did not always follow this pattern. On occasions isoprene levels stayed elevated in the morning despite a drop in temperature and associated increase in relative humidity and DMS. One explanation for this is an influence from a small forest upwind of the site. The Pikni forest 7 km to the southwest and some 300

Another interesting tracer for the influence of biogenic emissions is the sum of the oxidation products of isoprene (methacrolein, methyl vinyl ketone and isoprene peroxides measured at mass 71.0491 ~~m lower than the site can, given the right meteorological conditions, contribute to isoprene levels at the site despite its short lifetime (ca. 30 minutes~~ amu) which can be found in the midsection of Figure 5. The figure reveals that the level of the isoprene oxidation products, which is a function of the precursor isoprene mixing ratio and the OH concentration, was lower, but started to increase at the same time in the morning as the values of isoprene. MVK and MAC have a longer lifetime of 5-7 h with respect to ~~the removal by OH , using a mean OH concentration of 5~~OH ($2 \times 10^6$ molec $cm^{-3}$~~measured between 6 am and 10 am) . With an assumed average wind speed of 3.5 m/s the transport time of isoprenefrom the forest to the site would amount to ∼ 30 minutes. The same reasoning can be applied to the monoterpenes, because their lifetime amounts to ca. 60 min. with respect to the removal by OH (calculated for α-pinene and an OH concentration of 5 ×~~) than isoprene. This means that these compounds can be transported over longer distances than isoprene. But the main wind direction was SW (see Fig.1), which means that the analyzed air masses were transported over the ocean for at least 12 h before reaching the site (see section 3.2.4). Furthermore the Mediterranean Sea is not a major source of isoprene. Therefore, transport of the oxidation products over long distances can be excluded. Still, the simultaneous increase of isoprene and its oxidation products means that the photochemical oxidation already took place. Most probably the majority of isoprene originates from the 10 ~~6 molec $cm^{-3}$). But in contrast to the isoprene data, the median and mean mixing ratios of the total monoterpenes showed less discrepancy, which might indicate differences concerning the source behavior. One possible explanation could be that species with different emission patterns for isoprene and for monoterpenes were not co-located. If the Pikni forest for example would be dominated by isoprene emitting plants, its irregular influence on the site could cause discrepancies between median and mean values of isoprene while the monoterpenes would remain unaffected. Other reasons supposably exist, such as a different emission regulation. However, direct measurements to demonstrate such different primary emissions were not performed and the atmospheric concentration development indicates a clear light dependent emission regulation for monoterpenes as for isoprene with a very close relationship between isoprene and monoterpene production~~km strip of land between the ocean and the site. During that short transport period oxidation already began. After midday OH decreases rapidly which leads to the decline in the mixing ratio of the oxidation products.

In summary, the local vegetation produces modest emissions of reactive isoprene and monoterpenes. Their diel mixing ratio profiles are both light driven with a maximum around midday and slight variations can be traced back to changes in the local meteorology.

### 3.2 Oxygenated volatile organic compounds (OVOCs)

#### 3.2.1 Local impacts~~and transport processes~~

In contrast to the pronounced diel cycles and low mixing ratios found for the biogenic compounds the oxygenated VOCs showed relatively high values with comparatively little variation~~.~~, which can be seen in Fig. 7~~displays the mean diel cycles of acetone, methanol and acetic acid~~. Only acetic acid mixing ratios have pronounced diel cycles from the east and from the west. During specific nights the site was situated within the residual layer/free troposphere, which is explained in more detail in section 3.2.2. The plots shown in Fig. 7 contain only data measured when the site was within the the planetary boundary layer (PBL). It should be noted that the exclusion of the residual layer/free troposphere biases the data set to daytime measurements. For methanol and acetone there is no evidence of a consistently different diel cycle that can be related to local emission or photochemical production over the short strip of land between sea and site. The mixing ratios of these compounds are rather determined by emissions and photochemistry remote from the site. It becomes clear that the mean and median mixing ratios deviate in the morning ~~and afternoon as already discussed for isoprene. The same reasoning is likely to apply:~~ which can be explained by variable local meteorology~~leading to high values in the morning and afternoon on some days~~.

Methanol exhibited a maximum mean and median mixing ratio in the early morning. Since vegetation is an important daytime source of methanol ~~under light conditions~~ (Fall and Benson, 1996; Hüve et al., 2007) this increase could be explained by sunlight dependent plant emissions or by evaporation of methanol collected in dew. However, the production and emissions processes in plants are a matter of discussion (Folkers et al., 2008). ~~The median mixing ratios of acetic acid indicate that a weak diel cycle is present. The acetic acid mixing ratios (humidity corrected) reveal a pronounced diel cycle~~

An especially pronounced diel cycle of the acetic acid can be found between the 16 and 21 July, which is displayed in Fig. 8. In this part of the campaign a distinct anticorrelation between the acetic acid mixing ratios and humidity is apparent. Fog formation, which occurs under specific meteorological conditions, notably 100 % relative humidity (RH) in the presence of cloud condensation nuclei, leads to droplet sedimentation, so that soluble gases are largely removed. Acetic acid is more strongly affected than acetone and methanol, because the latter are a factor 143 and 22 less soluble, respectively (Sander, 2015). Uptake to droplets and sedimentation only occurs when 100 % relative humidity is reached and thus cannot explain the diel cycle of acetic acid at less than 100 % RH. ~~Three~~ Several other effects could play a role in this process: ~~first,~~ e.g. local photochemical production and loss of acetic acid, ~~second~~emission from and/or uptake by vegetation and soil, in-mixing from the residual layer/free troposphere by turbulence and~~third, emission from and~~/~~or uptake by vegetation and soil. The measured production from 06:00 till 14:00 and the loss rate from 14:00 till 22: 00 during the period from the~~ or fog bank formation below the site which was observed on

several occasions. To investigate this further the following formula was used to estimate the missing production rate for acetic acid around midday:

$$[Acid] = \frac{P_{res} + P_{OH}}{L_{OH} + L_{dep}} \quad (1)$$

$$P_{res} = [Acid] \times (L_{OH} + L_{dep}) - P_{OH} \quad (2)$$

where [Acid] refers to the mean acetic acid mixing ratio around midday , $P_{OH}$ to the photochemical production rate, $L_{OH}$ to the loss rate by the reaction with OH radicals, $L_{dep}$ to the dry deposition velocity. $P_{res}$ represents the residual production rate, which is the sum of several production terms such as emission from soil and vegetation as well as advection. The mean values at midday were determined from the diel cycles over the whole campaign. $L_{OH}$ was calculated by multiplying the mean value of OH around midday with its reaction rate constant with the acid, which gives a loss rate of 0.016 $h^{-1}$. The production rate $P_{OH}$ was calculated in the following way: average levels of acetaldehyde as the main precursor and of OH at midday and their reaction rate constant were multiplied, which gives the production rate of the acetyl peroxy radicals. Taking the measured concentrations of NO and $HO_2$ and their reaction rate constants with the acetyl peroxy radical into account it was found that the radical reacts to approximately 65 % with NO and 35 % with $HO_2$. It has been previously determined that 16~~to the 21 July amounted roughly to 0.1 ppbv/h and 0.08~~% of the reaction between acetyl peroxy radical and $HO_2$ produce acetic acid (Groß et al., 2014). Thus, the production rate for acetic acid amounts to 0.0082 ppbv~~/h, respectively. Sanhueza and Andreae (1991) reported a daily average emission of acetic acid from savanna soil of 0.07 nmol $m^{-2}$~~$h^{-1}$. This quite low production rate is consistent with the low level of PAA found. For the dry deposition velocity an area weighted average value of 0.427 ~~$s^{-1}$. Assuming a planetary boundary layer (PBL) height of 500~~ cm $s^{-1}$ was used, retrieved from the EMAC model. Ceilometer data from the site (height 650 m above sea level) revealed an average of 250 m ~~this would give a~~ for the PBL. Thus, the dry deposition velocity amounted to 0.061 ppbv $h^{-1}$. Applying these values leads to a remaining production rate of ~~0.012~~0.087 ppbv $h^{-1}$. ~~Although a direct comparison might be difficult, because the measurements were performed at different locations, the discrepancy of one order of magnitude strongly indicates that other processes than emission from soil played a role. According to Paulot et al. (2011), emissions from terrestrial vegetation account for 3~~Due to the high uncertainty in many of the applied values the error of $P_{res}$ amounts to ca. 133 %~~of the total sources while secondary photochemical production represents the major part of 69 %. However, in a remote site the contribution of secondary production is expected to be minor~~ .

Several effects give rise to the distinct diel profile in acetic acid. For example the term for dry

deposition becomes stronger in the evening due to a ~~lack of precursors. Thus, it was concluded that~~ decreasing boundary layer height. Furthermore concentrations of the OH radical change during the day, which results in variations in both production and loss rates. Additionally in-mixing from the ~~free troposphere contributed~~ residual layer/free troposphere could contribute to the net, apparent production ~~rate~~ with the onset of turbulent mixing in the morning. It ~~is assumed~~ was found that, in comparison to the PBL, acetic acid levels are elevated in the ~~free troposphere~~ residual layer/free troposphere (see section 3.2.2) due to the high deposition rate of the acid within the PBL. ~~The distinct diel cycles of acetic acid also coincided with a period of higher solar radiation (see Fig. 8), which promoted turbulence.Hartmann et al. (1991) determined a dry deposition rate of 0.5–1~~ However, the ceilometer data revealed that the entrainment velocity was very low during daytime (max. $\approx$ 1 cm $s^{-1}$ ~~for acetic acid in a savanna region. A boundary layer height of 500 m and an average acetic acid mixing ratio of 1 ppbv during the day would result in a loss rate of 0.04–0.07 ppbv/h. The measured loss rate in Cyprus (0.08 ppbv/h) was already quite close to these values, which suggests that dry deposition is the major loss process of acetic acid. The reason why acetic acid did not display diel variability during the whole campaign is related to varying meteorological conditions, e.g. in the periods associated with strong decreases in humidity the site was likely within the free troposphere at night so that no distinct diel cycles could be established. Furthermore long distance transport could have dominated over local processes.~~ ). Therefore we assume in-mixing plays only a minor role. Several times during the campaign an extensive fog bank formed below the site in the direction of advecting air. It is therefore concluded that acetic acid was scavenged within this fog bank, which was in close contact with the ground allowing deposition to occur. During the day the fog gradually dispersed which is concurrent with a slow increase in acetic acid mixing ratios caused both by evaporation from the fog and reduction in scavenging.

~

### 3.2.2 Transport processes and influence of the source region and the residual layer/free troposphere

To investigate the influence of transport processes the source regions and transport pathways of air arriving at the site were examined using the FLEXPART model. The area of influence of each single simulation can be described by the fraction of time the air has spent over different regions. For this study, the upwind region, namely the European continent, has been delineated into color coded sections, see Fig. 9, upper left panel. Thus, the overall transport time for air masses reaching the site can be subdivided in specific colored fractions between 0 and 1. As one single colorbar characterizes the transport history of air at a certain time step, the combination of all colorbars of all single simulations weighted by time results in an overview of the evolution of transport patterns. This is shown in upper part of the right panel of Fig. 9.

The lower part of the right panel of Fig. 9 shows for each simulation the fraction of the time the air has spent within the planetary boundary layer, where surface processes (e.g. surface emissions or

uptake of trace gases) can influence the air composition. This fraction lay between 10% and 35%. To determine the footprint for a spatially and temporally variable layer as the PBL it was necessary to consider the PBL height over time at each single column within the area of influence. For example the air mass that arrived on 21 July in Cyprus had spent 30 % of the last 120 h within the PBL (see lower panel on the right in Fig. 9). Of these 30 %, two thirds were affected by Eastern Europe, marked in red, purple and pink. In contrast, on the 25 July the air was 35 % of the time inside the PBL, whereof the main part was within marine boundary layer (MBL, marked in blue).

In the center section of the graph, mixing ratios of methanol ~~, acetone and acetic acid~~ and acetone are plotted on the same time scale. From Fig. 9 it can be seen that the mixing ratios of ~~all three~~ both compounds were higher when the air sampled came from Eastern Europe (red, purple, pink) and lower when arriving from western areas (shades of green). Transport from the West to Cyprus entails longer transport times in the Mediterranean marine boundary layer than from the East. The trend implies that either the sources in Eastern Europe were stronger or removal processes had a greater influence in air transported from the West.

~~In Table ?? campaign~~During specific periods of the campaign, ozone showed higher values at night than during the day while relative humidity dropped drastically (see Figure 10). These features indicate that the site was within the residual layer/free troposphere (e.g. Fischer et al., 2003). To separate the data the ozone values were multiplied by the mirrored relative humidity (100-RH). A threshold of 1000 ppbv·% was chosen as a criterion of being in the residual layer/free troposphere. Furthermore, only night time periods were considered, because ceilometer data and vertical profiles from radio sondes confirmed that the site was within the boundary layer during the day. At night the mixed layer height calculations from the ceilometer data are unreliable, due to weak vertical mixing and the incomplete optical overlap of the lidar signal at low heights (Haeffelin et al., 2012). The time periods identified as being within the residual layer/free troposphere are color coded in red in Figure 10. Table 1 separates the averaged mixing ratios of different VOCs, $O_3$ and CO~~are listed and separated by Eastern and Western air flow~~ , measured when sampling the residual layer/free troposphere and the PBL, additionally separated by east and west. It becomes clear that methanol, acetonitrile, acetone and acetic acid levels in the residual layer/free troposphere were higher than those measured in the PBL. Still, compared to the standard deviations, the differences are rather small, especially for acetone and acetic acid. When examining the data from the residual layer/free troposphere, a marked difference can be found between eastern and western flow regimes. Therefore it can be concluded that the source strength on the continents as well as the distance from the source to the site significantly influence the VOC levels.

In the following the influence of the source region is analyzed and only data within the PBL are regarded. Consistent with methanol, acetone and acetic acid, other OVOCs like acetaldehyde and methylethylketone as well as $O_3$ and CO show higher mixing ratios in air masses with Eastern European origin (see Table 1). The mixing ratio of acetonitrile, a tracer for biomass burning, was ~~ca.~~

between 100 and 110 pptv in both flow regimes. These low mixing ratios and the lack of variability indicates that no air masses influenced by recent biomass burning reached Cyprus in the period of measurement. Anthropogenic tracers, such as the aromatic compounds benzene, toluene and the xylenes, showed very low mixing ratios between ~~20 and 50~~5 and 35 pptv, which confirms the remote location of the site and the minor influence of local anthropogenic emissions. ~~This is also stressed by the small number of points which are above the detection limit (see Table ??).~~ The high standard deviations of these aromatic compounds can be traced back to some ~~rarely occurring~~ occasional spikes. The ozone mixing ratios of 60 - 70 ppbv are consistent with or even slightly higher than values found in Gerasopoulos et al. (2005) and Kleanthous et al. (2014). The values measured during CYPHEX also exceed the European Air Quality Standard of 120 $\mu$g m$^{-3}$ (60 ppbv as a maximum daily 8 h mean)[4].

In the ~~following~~ next section we examine the role of photochemical processes on the mixing ratios of the OVOCs.

~~Hartmann1991~~

### 3.2.3 Investigation of photochemical processes using the CAABA/MECCA box model

The CAABA/MECCA box model was used to examine the photochemical processes influencing the mixing ratios of acetone ~~, acetic acid~~ and methanol. In order to simulate conditions in the MBL, where no major sources can be found, only initial values of precursors were set, with further emissions during the run deactivated, except for ozone. Dry deposition was also excluded, because this model run was intended to investigate photochemistry only. The trace gases included, their initial values (which originate from the Mainz Organics Mechanism (MOM) chemistry in the EMAC model (Jöckel et al., 2016)) as well as the chemical degradation scheme can be found in the supplement (S2 and S4). The model mixing ratios cannot be directly compared to the results of section 3.2.1, because processes like transport, ocean emission/uptake or dry deposition were not included in the box model. In Fig. 11 the predicted mixing ratios of methanol ~~, acetone and acetic acid~~ and acetone are displayed for a 48 h model run with an initial value for NOx of 2.4 ppbv. While methanol ~~and acetic acid decrease~~decreases, the mixing ratio of acetone increases. ~~Figures ??, ?? and ?? display the rates of important reactions with a production or loss rate $\geq 10^{-16}$ mol mol$^{-1}$ s$^{-1}$ (0.36 pptv/h) impacting the budgets of the OVOCs. The~~ The analysis revealed that the main process affecting methanol is the degradation by OH radicals. ~~For acetic acid, production via the peroxy acetyl radical ($CH_3C(O)O_2$) is countered by its loss via reaction with OH. Net production of acetic acid can be achieved only if enough organic precursors are emitted at low NOx level (ca. 300 pptv), which reduces the OH mixing ratio.~~ The modeled behavior of acetone is more complex. Among the most important reactions are its loss by OH radical reaction or photolysis as well as its production via the reaction of different intermediates, mainly peroxy radicals, with NO or OH, for example the reaction of isopropyl peroxy

[4]http://ec.europa.eu/environment/air/quality/standards.htm; accessed ~~11 July 2016~~26 April 2017

radicals ($iC_3H_7O_2$) with NO. Figures showing the rates of important reactions with a production or loss rate $> 10^{-16}$ mol mol$^{-1}$ s$^{-1}$ (0.36 pptv/h) can be found in the supplement S3. It can be concluded that secondary production in the MBL plays only a role for acetone, while methanol ~~and acetic acid are rather depleted~~is only lost.

### 3.2.4 Influence of marine boundary layer transport on OVOCs

In Fig. 12 mixing ratios of methanol ~~, acetone, and acetic acid~~ and acetone are plotted against the time the air spent in the marine boundary layer, calculated by adding up the FLEXPART modeled percentage of the influence of the Eastern and Western Mediterranean, the Black Sea, the Caspian Sea and the Atlantic Ocean. The summed percentage was then multiplied by the duration of the modeled backward trajectories (120 h). The data were separated into periods affected by Eastern and by Western Europe. The ~~$r^2$ values vary from 0.2–0.5, but the slopes were consistently negative in all cases, and steeper for air masses from Eastern Europe. The OVOCloss rate values amounted to 0.1~~blue markers refer to the data measured within the PBL, while the red markers represent data recorded while the site was within the residual layer/free troposphere. Since this analysis concentrates on the phenomena occurring within the boundary layer, the focus will be placed on the data measured in the PBL, only. However, it needs to be kept in mind that the air measured when being in the PBL has been influenced by the residual layer/free troposphere as well as the boundary layer during transport. An exponential fit was applied on the blue colored data points using the function:

$$[OVOC]_t = [OVOC]_0 \times exp(-A \times t) \quad (3)$$

$[OVOC]_0$ represents the value in ppbv that would be measured at the source, t is the time in h and A is the loss rate constant in h$^{-1}$. The initial methanol and acetone values at the source ($[OVOC]_0$) yield 5.2 $\pm$ 0.3 ppbv ~~/hfor methanol , 0.06~~and 3.5 $\pm$ 0.2 ppbv ~~/h for acetone and 0.05~~from the east and 4.6 $\pm$ 0.5 ppbv ~~/h for acetic acid for the Eastern outflow and 0.06~~and 2.7 $\pm$ 0.2 ppbv ~~/h for methanol, 0.02~~from the west, respectively. These results show that the source strength for acetone is slightly larger in Eastern Europe than in Western Europe, while the initial values for methanol are consistent within the error range. Still, the trend also indicates a larger source strength for methanol from the East. The loss rate constants for methanol and acetone amount to 0.031 $\pm$ 0.004 ~~ppbv/h for acetone and 0.03~~h$^{-1}$ and 0.022 $\pm$ 0.003 ~~ppbv/h for acetic acid for a flow from the West. The net effect of transport~~ h$^{-1}$ from eastern air masses and 0.029 $\pm$ 0.005 h$^{-1}$ and 0.014 $\pm$ 0.003 h$^{-1}$ from western air masses, respectively. These loss rate constants over water for ~~all three substances is~~ the two substances are a function of dilution (by vertical and horizontal mixing), photochemical degradation, uptake or emission by the ocean and production from the oxidation of larger organic molecules. As already mentioned the atmospheric lifetimes with respect to the removal by OH radicals were about 6 days for methanol ~~,~~ and 32 days for acetone~~and 8 days for acetic acid~~. FLEXPART calculated

transport times from Eastern Europe to Cyprus of roughly 12 h to 2 days and from Western Europe to the site of around 2–5 days. ~~Clearly the~~ The atmospheric lifetimes of acetone ~~, methanol and acetic acid are all~~ and methanol are relatively long compared to the average transport time. This allows the influence of the MBL to be gauged. ~~Only acetic acid was impacted by local effects in the period from 16–21 July, shown by its diel cycle. Since this period coincides with an Eastern flow regime, only air masses from Western Europe were investigated in the following study. The loss rates of the three~~ The losses of the two OVOCs were calculated using the ~~subsequent formula:~~ formula:

$$[OVOC]_t = [OVOC]_0 \times exp(-(k_{OH} \times [OH] + V_{dep}/H_{PBL}) \times t) \quad (4)$$

$$[RH]_t = [RH]_0 \times exp(-(k_{OH} \times [OH] + V_{dep}) \times t)$$

where [~~RH~~OVOC]$_t$ is the mixing ratio of the compound at a specific transport time t, [~~RH~~OVOC]$_0$ the mixing ratio ~~at the starting point of the linear fit~~ determined by the y axis intercept of the exponential fit of the measured data (PBL only), $k_{OH}$ the rate coefficient for the reaction with OH radicals, [OH] the ~~mixing ratio~~ concentration of the OH radicals~~and~~ , $V_{dep}$ the dry deposition ~~rate~~velocity and $H_{PBL}$ the height of the PBL. Photolysis rates are so low that they can be neglected, in fact the ground level photolysis rate of acetone is at least ten times lower than the loss rate due to OH. The diel averaged [OH] ~~mixing ratio~~ concentration at the site was measured during the CYPHEX campaign as $2 \times 10^6$ molec cm$^{-3}$. $k_{OH}$ values originate from IUPAC (Atkinson et al., 2006). Since OH concentrations were constrained by measurement with an accuracy of 28.5 % (further analysis see gray dashed line in Fig.12) and the OH rate coefficients are well known this loss term is assumed to be reasonably accurate. Dry deposition ~~rates~~velocities, on the other hand, represent a large uncertainty factor and dilution by vertical and horizontal mixing is not accounted for in the equation. ~~Three different scenarios are considered here:Dry deposition rates~~ The deposition velocities simulated in EMAC (Jöckel et al., 2016) over the Mediterranean ~~sea~~ Sea were taken and the area weighted average values amounted to~~0.41 cm s$^{-1}$ for acetic acid, 0.031~~0.030 cm s$^{-1}$ for acetone and ~~0~~$1 \times 10^{-4}$ cm s$^{-1}$ for methanol despite the higher solubility of methanol in comparison to acetone. The values are net deposition velocities calculated in a resistant-type scheme based on Wesely (1989) and implemented by Kerkweg et al. (2006), so they ~~may not proportionate~~ do not need to be proportional to the solubilities of the species. ~~An~~ As already mentioned, ceilometer data from the site gave a PBL height of 250 m. This PBL was actually an internal boundary layer, that formed inside the marine boundary layer due to thermal and orographic effects, as it was advected over land. For the boundary layer over sea relevant to this study, an average PBL height of 500 m was assumed. ~~The results~~ Previous aircraft studies in the region (Holzinger et al., 2005) focused on acetonitrile have reported vertical profiles over the sea that show sharp decreases in mixing ratios from 500 m to 250 m supporting the 500 m boundary layer over sea assumption made here. The decreases of acetone and methanol calculated

using equation 4 can be found as ~~light blue~~ black lines in Fig. 12. The ~~black~~ gray dashed lines refer to the calculated result when a 28.5 % higher OH concentration is applied, to account for the OH measurement uncertainty. The blue lines represent the ~~linear~~ exponential fit of the ~~measured data~~ data measured within the PBL. It becomes clear that ~~acetic acid is well captured by the calculation while~~ the measured net loss was ~~greater~~ larger than the calculated loss for methanol and acetone. ~~In the second scenario dry deposition rates were adjusted so that the measured loss rates were reached. This method yielded a dry deposition rate constant of 0.21 cm $s^{-1}$ for methanol, 0.10 cm $s^{-1}$ for acetone and 0.42 cm $s^{-1}$ for acetic acid, still assuming a PBL height of 500 m. These values do not reflect the relative solubilities. According to Sander (2015) methanol has a Henry's Law constant between 1.7 and 2.2 mol $m^{-3}$ $Pa^{-1}$, acetone between 0.26 and 0.33 mol $m^{-3}$ $Pa^{-1}$ and acetic acid between 40 and 46 mol $m^{-3}$ $Pa^{-1}$. Based on solubility alone we would therefore expect the acetic acid loss rate to be much higher than that of acetone. In the last scenario the dry deposition of methanol was adjusted so that the loss rate matches the measured one (0.21 cm $s^{-1}$). The dry deposition rates of acetic acid and acetone were set according to their relative solubilities: 4.4 cm $s^{-1}$ for acetic acid and 0.031 cm $s^{-1}$ for acetone. The results can be found as violet lines in Fig. 12. Interestingly the value for acetone gained by this method is the same as in the model and its loss rate is still underestimated. The loss rate of acetic acid is now even higher than the measured one. Clearly, the measured loss rates of methanol and acetone are higher than expected. Although the acetic acid loss rate is nicely reproduced by the model, a higher loss rate would be anticipated owing to its solubility. Four possible explanations for this apparent anomaly will be considered here. The first is that~~ Since the difference in slope of the black and gray lines is much smaller than the difference to the measured data, it can be concluded that the loss through oxidation by OH only plays a minor role. To explain the general trend that the calculation underestimates the loss of acetone and methanol over the ocean five effects need to be taken into account: Firstly, vertical transport to the sea surface layer was a limiting factor, so that turbulence rather than solubility defined the distribution. ~~The second is that sea-water surface layer concentrations of acetic acid were high relative to methanol and acetone, compensating for the difference in solubilities. The third is that photochemical production of acetic acid in air was much more influential than that of acetone and methanol. The fourth is that~~ Secondly, microbial consumption and/or production is a missing sink, thirdly photochemical production played a role, fourthly in-mixing of air from the ~~free troposphere is significant~~ residual layer/free troposphere was significant and fifthly the variability in the emissions at the source had a considerable influence.

A turbulence driven distribution can be the reason why the ~~loss rates~~ losses do not represent the solubilities of the ~~three~~ two OVOCs, but it cannot explain the discrepancy between the measured and the calculated loss ~~rates~~ rate constants of methanol and acetone.~~Other explanations need to be consulted.~~

~~Although ocean~~ Ocean concentrations and air-sea fluxes of acetone and methanol have been determined previously (Williams et al., 2004; Sinha et al., 2007) ~~, to our knowledge no equivalent~~

measurements for acetic acid exist. Generally and it has been found for methanol and acetone that the ocean and air are close to equilibrium on a global scale (Millet et al., 2008; Fischer et al., 2012), but that a significant aqueous phase production term exists for both species. Regionally, strong biological activity can drive a surface ocean oversaturation of acetone that leads to its emission (Taddei et al., 2009). Dixon et al. (2014) have shown that methanol is more efficiently consumed microbially than acetone. One reason for the higher loss rate constant of methanol in comparison to acetone could therefore be the higher oxidation rate of methanol in the ocean. Since no microbiological influence is included in the calculation, a consumption of both acetone and methanol by microorganisms could explain the higher measured loss rate constant.

Significant in-situ photochemical production would also lead to an underestimation of loss rates.Estimates of global budgets of the three OVOCs reveal that photochemical production is larger for acetic acid relative to methanol and acetone (Millet et al., 2008; Paulot et al., 2011; Fischer et al., 2012). However, the CAABA/MECCA box model indicates that acetic acid is depleted The boxmodel has shown that acetone is weakly photochemically produced over the ocean rather than produced due to a lack of precursors (see section 3.2.3). The model results for acetone on the other hand showed a slight production. Therefore, photochemical production would increase to some extent. If a photochemical production term would be included in the formula, then the discrepancy between observed and expected loss rates for acetic acid and for acetonethe calculation and the measurement would be even higher. Thus, photochemical production can not be the missing factor.

Another possible reason for the high loss rates rate constants could be in-mixing of acetone and methanol poor air from the residual layer/free troposphere. That in-mixing took place or that But the data measured when the site was even within the free troposphere is confirmed by strong decreases in humidity levels (see Fig. 8) and by the loss rate of CO. In general no significant loss of CO is assumed over the ocean due to its long lifetime of ca. 40 days with respect to the removal by OH and its negligible dry deposition.However, a loss rate within the residual layer/free troposphere have shown, that levels of 0.65 ppbv/h, which is higher than expected, was determined.the two OVOCs were elevated above the boundary layer, so that acetone and methanol rich air would have been entrained. Additionally, the marine boundary layer is expected to be rather stable due to the high pressure system over the Mediterranean. Thus, it can be concluded that entrainment of air from the free troposphere occurred. If dry deposition rates reflecting the solubilities are assumed, it would therefore mean that acetic acid rich air caused a reduction in its net loss rate. As discussed above, a higher mixing ratio of acetic acid in the free troposphere is reasonable due to its high deposition loss rate in the PBL. The most likely explanation for our observations are that vertical entrainment impacted on the mixing ratios measured downwind of the source regions. Furthermore microbial consumption within the sea surface layer could play a role . in-mixing cannot explain the difference between measurement and calculation.

Furthermore, the spatially variable emissions on the continents might also be temporally correlated

which can influence the measured loss rate constants.
The most plausible explanation for the discrepancy is therefore a combination of a missing sink for methanol and acetone in the ocean, possibly enhanced by microbial consumption, and spatial and temporal variability of the emissions in the source regions.
Dry deposition velocities, that would be necessary to match the measured data, amount to 0.34 cm $s^{-1}$ for methanol and 0.28 cm $s^{-1}$ for acetone in air masses from the East and 0.31 cm $s^{-1}$ for methanol and 0.18 cm $s^{-1}$ for acetone from a western flow regime. It is expected that the results for the dry deposition velocities are independent of the origin of the air mass. This is roughly the case for methanol, but the acetone data require a lower dry deposition velocity for western than for eastern air masses. The reason for that could be that photochemical production of acetone, which was not included in the theoretical formula, plays a role and was different for eastern and western air masses. If the photochemical production would be implemented in the formula, an even higher value for the dry deposition velocity would be necessary so that the result would still match the measured data.

### 3.2.5 Correlations between acetone, methanol, ~~acetic acid,~~ CO and ozone

Table 2 shows slopes, intercepts and correlation coefficients ($r^2$) from the bivariate fits between methanol, acetone, ~~acetic acid,~~ CO and ozone separated by eastern and western air masses. ~~In~~ Two spikes in the acetone data ~~the two spikes~~ (occurring at the 24 July and 2 August) and one spike in the CO data were removed, because they were most probably emerging from local sources. The correlations were calculated using the data measured within the PBL, only. It can be seen that ~~the correlations calculated from air masses originating in Eastern Europe are, on average, higher than the ones from Western Europe~~acetone and methanol correlate reasonably well, while the correlation factor is higher in eastern than western air masses. As already mentioned horizontal or vertical dilution/ in-mixing, photochemical processes as well as emission or uptake by the ocean play important roles during transport. These effects can influence the various compounds to different degrees, so that divergent correlation factors are expected. ~~Figure ?? displays the correlations between the OVOCs divided into eastern and western flow regimes. The decreasing correlation factors appear as higher scatter between the trace-gases measured in western air masses. The highest correlation was found between acetone and acetic acid in the eastern flow ($r^2$=0.81), while in the western flow the correlation between the same molecules, acetone and acetic acid, yields $r^2$=0.52, only. The slope between acetone and acetic acid on the other hand stayed almost the same for both flow regimes (~1). However, the graph referring to air coming from Western Europe shows two rather distinct branches. This can be understood if acetone and acetic acid were influenced by different loss~~ A good correlation can be interpreted by a co-location of sources and/or ~~production processes that lead to the grouping of the data points along different correlation lines and the decreasing $r^2$ value. The longer the transport time the more important are the discrepancies between loss and production. To~~

a lesser degree, similar effects are found in the correlation between methanol and acetone. Here the correlation factors decreased from 0.76 (eastern flow) to 0.62 (western flow). In Figure ?? correlations similar production and depletion processes. No correlation was found between methanol and acetone as well as acetic acid from western flow regimes are color coded by relative humidity and $O_3$. The methanol vs. acetone ozone as well as acetic acid vs. acetone plots color coded by RH reveal that the origin of the different branches is tied into high relative humidity and thus fog events (RH > 90 %, black dots). Since methanol and acetic acid are more soluble than acetone , these compounds are more efficiently removed by droplet sedimentation in foggy conditions. This leads to a decrease in the slope and therefore the formation of the lowest branch. Furthermore, the acetic acid vs. acetone plot color coded by $O_3$ shows that higher ozonelevels were correlated with higher acetic acid and/or lower acetone mixing ratios. The branching was most probably dominated by the relationship between acetic acid and ozone, because there was no correlation between acetone and ozone in the western flow regime ($r^2$=0.04). Since ozone is in general generated by photochemical processes, the correlation may indicate that acetic acid is also generated photochemically, which would however contrast the conclusions of the box-model study (see section 3.2.3) in which acetic acid is lost rather than formed over the ocean due to a lack of precursors. Another reason for the correlation could be in-mixing of both compounds from the free troposphere as both acetic acid and $O_3$ mixing ratios are expected to decrease close to the ground due to dry deposition. Another indication for the impact of air masses from the free troposphere is the low relative humidity. The high ozone mixing ratios (color coded in yellow) coincide with RH levels below 70 % (color coded in blue), which can be interpreted that rather dry, but ozone rich air was influencing the site.The correlation coefficients between acetic acid and methanol, listed in Table 2, showed no difference between eastern and western air masses, but the slope slightly decreased when changing from eastern to western flow regimes. If only the loss rates over the ocean are taken into account (see Fig. 12 and section 3.2.4) an increasing instead of decreasing slope would be expected, because acetic acid showed a weaker decline than methanol. The slope between methanol and acetone on the other hand increased when changing from eastern to western air masses, although a decrease would be expected. But the slopes are in general dominated by high values originating from air masses that stayed a comparatively short time in the MBL. Hence, other effects played an important role, e.g. different emission ratios on the continent, local impacts like fog events or changing meteorological conditions. Especially acetic acid was biased by these local effects during an eastern flow regime which can be seen in the diel cycles between the 16 acetone and 21 July (see section 3.2.1) ozone. Comparing the three The reason are the different sources: ozone is secondarily produced during the transport, while the other two compounds have strong sources on the continent and decrease (methanol) or only slightly increase (acetone) during transport processes. Comparing the two OVOCs to CO (Table 2) shows that the slope as well as the correlation between methanol and CO remained remarkably as well as acetone and CO remained fairly constant between the western and eastern eastern and western flow

regimes (~~slope~~methanol: slope =~~0.067 and 0.065~~ 0.061 and 0.070, $r^2$ = 0.45 and 0.44, respectively; acetone: slope = 0.038 and 0.037, $r^2$ = 0.59 and ~~0.45~~0.65, respectively ). ~~In contrast to acetic acid and acetone, this correlation appears to be~~ These correlations appear to be rather insensitive to the combined processes of dilution, marine uptake/emission and photochemical ageing for air masses in this region. The data can be compared to the MINOS campaign, which took place 13 years before in Finokalia, Crete (Salisbury et al., 2003). One part of the MINOS campaign, with no biomass burning influence and an eastern flow regime ("period 1"), was the most appropriate to compare to the CYPHEX data. Interestingly, the ratio between methanol and CO calculated from Salisbury et al., (2003) (0.02 for "period 1") is smaller than the one determined in this study (~~0.033~~0.031). The reason for this is a lower CO mixing ratio (MINOS: 167 ppbv, CYPHEX: 107 ppbv), while the methanol values were similar in both campaigns (MINOS: 3.34 ppbv, CYPHEX: ~~3.54~~ 3.33 ppbv). In the same way, the acetone/CO ratio measured in this study (~~0.025~~0.024) for easterly conditions was larger than the one reported by Salisbury et al., (2003) (0.017, "period 1") due to lower CO mixing ratios. The decreased CO values might be traced back to the economic crisis in Greece, which led to a reduction of industrial production and therefore to decreasing emissions of anthropogenic compounds like CO. ~~Another interesting relationship arose between ozone and the OVOCs. Regarding western air masses the correlations between the OVOCs and ozone were extremely poor, the best being between acetic acid and $O_3$ ($r^2$=0.25), while the others were below $r^2$=0.01. In eastern flow regimes, on the other hand, the correlations were slightly stronger. If the correlation plots among the OVOCs from eastern air masses are color coded by ozone (Fig. **??**), it can be seen that all plots show the same pattern: the higher the ozone values the higher the OVOC mixing ratios. This can be explained by the shorter distance from Cyprus to the sources in Eastern Europe. Still, it needs to be kept in mind that the sources for the four compounds are different, e.g. methanol is mainly biogenically produced while secondary photochemical production dominates for acetic acid over land. The reason for the correlation could simply be that the sources were co-located on the continent and due to the shorter transport time from Eastern Europe the various loss and production processes had a weaker impact than in air masses from Western Europe.~~

## 4 Summary

During the 2014 CYPHEX campaign, trace gases in air masses from Eastern (67 % of the time) and Western Europe (33 % of the time) were ~~measured~~monitored. Since the transport routes of the air pass over the Mediterranean Sea the impact of the marine boundary layer on ~~VOCs and especially~~ OVOCs could be investigated. Due to the sparse vegetation local biogenic emissions of isoprene and monoterpenes were weak~~(always <350 pptv)~~. These species showed typical diel cycles with the highest mixing ratios around midday. The difference in median and mean mixing ratios in the isoprene data could be explained by the boundary layer evolution ~~,~~ and the onset of a local sea breeze

systemand the presence upwind of a small forest in the southwesterly wind direction. The methanol and acetone mixing ratios revealed relatively little diel variation, but higher absolute mixing ratios, indicating that local emission or production was less significant in comparison to long range transport. Only acetic acid followed a pronounced diel cycleduring one period of the campaign, which is the result of various local effects like emissionfrom soil, in-mixing from the free troposphere due to turbulence as well as dry and wet net effect of photochemical production and loss, direct emission, dry deposition over land . The lack of diel cycles during the rest of the campaign can be explained by a higher impact of transport processes and different meteorological conditions. To exclude these local phenomena only data measured from western air masseswere used to investigate the influence of the MBL during transportand in-cloud scavenging from advecting air masses. The methanol , acetone and acetic acid and acetone data showed that uptake to the sea surface was not defined solely by solubility and that vertical entrainment likely played an important rolethe discrepancy between measured and calculated loss rate constant can potentially be explained by a missing sink in the Mediterranean Sea and a emission variability in the source region. The correlation coefficients between the OVOCs were higher in eastern than in western air masses, which can be explained by the longer transport time over the ocean and thus stronger impacts of different production and loss processes in the western flow regimeas well as some local effects like fog formation. The ratios of methanol/CO and acetone/CO were higher in this work than in a study performed over a decade ago13 years before, consistent with the lowering in the regional sources of CO. The results displayed here indicate that air reaching Cyprus from Eastern and Western Europe showed different OVOC characteristics due to different emission patterns, transport times as well as varying impact of photochemical processes, dilution and ocean uptake or emission.

## Author contribution

B. Derstroff performed the PTR-TOF-MS measurements and prepared the manuscript with contributions from J. Williams, J. N. Crowley., H. Fischer, J. Kesselmeier and the other co-authors. I. Hüser and H. Harder provided the data of the FLEXPART model, R. Sander instructed the application of the CAABA/MECCA box model. CO and ozone measurements were performed by U. Parchatka and monoterpene measurements by E. Bourtsoukidis. Peracetic acid data were provided by G. J. Phillips and J. N. Crowley, photolysis rates by J. Schuladen, dry deposition rates from the EMAC model by S. Gromov and OH concentrations by C. Mallik and H. Harder. J. N. Crowley and J. Lelieveld designed the study. C. Sauvage, C. Stönner, A. Novelli, L. Tomsche and M. Martinez carried measurements out in Cyprus.

The authors declare that they have no conflict of interest.

## Data availability

The data set is available from the CYPHEX server on request. If desired, please send an email to jonathan.williams@mpic.de

*Acknowledgements.* We would like to thank our engineers Thomas Klüpfel and Rolf Hofmann for their help and support. Furthermore we thank the Cyprus Ministry of Defense for the use of the base of the National Guard at Ineia and the generous assistance of the Lara Naval Observatory staff. Our thanks also go to the Department of Labor Inspection for helping us set up the campaign. Additionally we would like to thank Laurens Ganzeveld for inspiring discussions.

## References


European Commission, http://ec.europa.eu/environment/air/quality/standards.htm, accessed 11 July 2016.

Populationlist, http://www.populationlist.com/Eparchia_Pafou/06/760931/state\T1\textendashpopulation, accessed on 16 August 2016.

Worldbank, http://data.worldbank.org/country/cyprus, accessed on 4 May 2016.

Arnold, S. R., Spracklen, D. V., Williams, J., Yassaa, N., Sciare, J., Bonsang, B., Gros, V., Peeken, I., Lewis, A. C., Alvain, S., and Moulin, C.: Evaluation of the global oceanic isoprene source and its impacts on marine organic carbon aerosol, Atmos. Chem. Phys., 9, 1253–1262, doi:10.5194/acp-9-1253-2009, http://www.atmos-chem-phys.net/9/1253/2009/, 2009.

Atkinson, R.: Gas-phase tropospheric chemistry of organic compounds: A review, Atmos. Environ., 24, 1–41, doi:10.1016/0960-1686(90)90438-S, http://www.sciencedirect.com/science/article/pii/096016869090438S, 1990.

Atkinson, R., Baulch, D. L., Cox, R. A., Crowley, J. N., Hampson, R. F., Hynes, R. G., Jenkin, M. E., Rossi, M. J., Troe, J., and Subcommittee, I.: Evaluated kinetic and photochemical data for atmospheric chemistry: Volume II - gas phase reactions of organic species, Atmos. Chem. Phys., 6, 3625–4055, doi:10.5194/acp-6-3625-2006, http://www.atmos-chem-phys.net/6/3625/2006/, IUPAC Task Group on Atmospheric Chemical Kinetic Data Evaluation, http://iupac.pole-ether.fr, accessed on 12 July 2016, 2006.

Baasandorj, M., Millet, D. B., Hu, L., Mitroo, D., and Williams, B. J.: Measuring acetic and formic acid by proton transfer reaction-mass spectrometry: sensitivity, humidity dependence, and quantifying interferences, Atmos. Meas. Tech. Discuss., 7, 10 883–10 930, doi:10.5194/amtd-7-10883-2014, http://www.atmos-meas-tech-discuss.net/7/10883/2014/, 2014.

Bonsang, B., Polle, C., and Lambert, G.: Evidence for marine production of isoprene, Geophys. Res. Lett., 19, 1129–1132, doi:10.1029/92GL00083, http://dx.doi.org/10.1029/92GL00083, 1992.

Broadgate, W. J., Liss, P. S., and Penkett, S. A.: Seasonal emissions of isoprene and other reactive hydrocarbon gases from the ocean, Geophys. Res. Lett., 24, 2675–2678, doi:10.1029/97GL02736, http://dx.doi.org/10.1029/97GL02736, 1997.

Cline, J. D. and Bates, T. S.: Dimethyl sulfide in the Equatorial Pacific Ocean: A natural source of sulfur to the atmosphere, Geophys. Res. Lett., 10, 949–952, doi:10.1029/GL010i010p00949, http://dx.doi.org/10.1029/GL010i010p00949, 1983.

Davison, B., Taipale, R., Langford, B., Misztal, P., Fares, S., Matteucci, G., Loreto, F., Cape, J. N., Rinne, J., and Hewitt, C. N.: Concentrations and fluxes of biogenic volatile organic compounds above a Mediterranean macchia ecosystem in western Italy, Biogeosciences, 6, 1655–1670, doi:10.5194/bg-6-1655-2009, http://www.biogeosciences.net/6/1655/2009/, 2009.

Dixon, J. L., Beale, R., Sargeant, S. L., Tarran, G. A., and Nightingale, P. D.: Microbial acetone oxidation in coastal seawater, Front. Microbiol., 5, doi:10.3389/fmicb.2014.00243, http://doi.org/10.3389/fmicb.2014.00243, 2014.

Doche, C., Dufour, G., Foret, G., Eremenko, M., Cuesta, J., Beekmann, M., and Kalabokas, P.: Summertime tropospheric-ozone variability over the Mediterranean basin observed with IASI, Atmos. Chem. Phys., 14, 10 589–10 600, doi:10.5194/acp-14-10589-2014, http://www.atmos-chem-phys.net/14/10589/2014/, 2014.

Fall, R. and Benson, A. A.: Leaf methanol — the simplest natural product from plants, Trends Plant Sci., 1, 296 – 301, doi:10.1016/S1360-1385(96)88175-0, http://www.sciencedirect.com/science/article/pii/S1360138596881750, 1996.

Feilberg, A., Liu, D., Adamsen, A. P. S., Hansen, M. J., and Jonassen, K. E. N.: Odorant Emissions from Intensive Pig Production Measured by Online Proton-Transfer-Reaction Mass Spectrometry, Environ. Sci. Technol., 44, 5894–5900, doi:10.1021/es100483s, http://dx.doi.org/10.1021/es100483s, 2010.

Fischer, E. V., Jacob, D. J., Millet, D. B., Yantosca, R. M., and Mao, J.: The role of the ocean in the global atmospheric budget of acetone, Geophys. Res. Lett., 39, doi:10.1029/2011GL050086, http://dx.doi.org/10.1029/2011GL050086, 2012.

Fischer, H., Kormann, R., Klüpfel, T., Gurk, C., Königstedt, R., Parchatka, U., Mühle, J., Rhee, T. S., Brenninkmeijer, C. A. M., Bonasoni, P., and Stohl, A.: Ozone production and trace gas correlations during the June 2000 MINATROC intensive measurement campaign at Mt. Cimone, Atmos. Chem. Phys., 3, 725–738, doi:10.5194/acp-3-725-2003, http://www.atmos-chem-phys.net/3/725/2003/, 2003.

Folkers, A., Hüve, K., Ammann, C., Dindorf, T., Kesselmeier, J., Kleist, E., Kuhn, U., Uerlings, R., and Wildt, J.: Methanol emissions from deciduous tree species: dependence on temperature and light intensity, Plant Biology, 10, 65–75, doi:10.1111/j.1438-8677.2007.00012.x, http://dx.doi.org/10.1111/j.1438-8677.2007.00012.x, 2008.

Galbally, I. and Kirstine, W.: The Production of Methanol by Flowering Plants and the Global Cycle of Methanol, J. Atmos. Chem., 43, 195–229, doi:10.1023/A:1020684815474, http://dx.doi.org/10.1023/A%3A1020684815474, 2002.

Gerasopoulos, E., Kouvarakis, G., Vrekoussis, M. and. Kanakidou, M., and Mihalopoulos, N.: Ozone variability in the marine boundary layer of the eastern Mediterranean based on 7-year observations, J. Geophys. Res., 110, doi:10.1029/2005JD005991, http://dx.doi.org/10.1029/2005JD005991, 2005.

Graus, M., Müller, M., and Hansel, A.: High Resolution PTR-TOF: Quantification and Formula Confirmation of VOC in Real Time, J. Am. Soc. Mass. Spectrom., 21, 1037–1044, doi:10.1016/j.jasms.2010.02.006, http://www.sciencedirect.com/science/article/pii/S1044030510001005, 2010.

Groß, C. B. M., Dillon, T. J., Schuster, G., Lelieveld, J., and Crowley, J. N.: Direct Kinetic Study of OH and O3 Formation in the Reaction of CH3C(O)O2 with HO2, J. Phys. Chem., 118, 974–985, doi:10.1021/jp412380z, http://dx.doi.org/10.1021/jp412380z, 2014.

Haase, K. B., Keene, W. C., Pszenny, A. A. P., Mayne, H. R., Talbot, R. W., and Sive, B. C.: Calibration and intercomparison of acetic acid measurements using proton-transfer-reaction mass spectrometry (PTR-MS), Atmos. Meas. Tech., 5, 2739–2750, doi:10.5194/amt-5-2739-2012, http://www.atmos-meas-tech.net/5/2739/2012/, 2012.

Haeffelin, M., Angelini, F., Morille, Y., Martucci, G., Frey, S., Gobbi, G. P., Lolli, S., O'Dowd, C. D., Sauvage, L., Xueref-Rémy, I., Wastine, B., and Feist, D. G.: Evaluation of Mixing-Height Retrievals from Automatic Profiling Lidars and Ceilometers in View of Future Integrated Networks in Europe, Boundary-Layer Meteorology, 143, 49–75, doi:10.1007/s10546-011-9643-z, http://dx.doi.org/10.1007/s10546-011-9643-z, 2012.

Hens, K., Novelli, A., Martinez, M., Auld, J., Axinte, R., Bohn, B., Fischer, H., Keronen, P., Kubistin, D., Nölscher, A. C., Oswald, R., Paasonen, P., Petäjä, T., Regelin, E., Sander, R., Sinha, V., Sipilä, M., Taraborrelli, D., Tatum Ernest, C., Williams, J., Lelieveld, J., and Harder, H.: Observation and modelling

of $HO_x$ radicals in a boreal forest, Atmos. Chem. Phys., 14, 8723–8747, doi:10.5194/acp-14-8723-2014, http://www.atmos-chem-phys.net/14/8723/2014/, 2014.

Holzinger, R., Williams, J., Salisbury, G., Klüpfel, T., de Reus, M., Traub, M., Crutzen, P. J., and Lelieveld, J.: Oxygenated compounds in aged biomass burning plumes over the Eastern Mediterranean: evidence for strong secondary production of methanol and acetone, Atmos. Chem. Phys., 5, 39–46, doi:10.5194/acp-5-39-2005, http://www.atmos-chem-phys.net/5/39/2005/, 2005.

Hüve, K., Christ, M. M., Kleist, E., Uerlings, R., Niinemets, Ü., Walter, A., and Wildt, J.: Simultaneous growth and emission measurements demonstrate an interactive control of methanol release by leaf expansion and stomata, J. Exp. Bot., 58, 1783–1793, doi:10.1093/jxb/erm03, http://jxb.oxfordjournals.org/content/early/2007/03/20/jxb.erm038, 2007.

Jöckel, P., Tost, H., Pozzer, A., Kunze, M., Kirner, O., Brenninkmeijer, C. A. M., Brinkop, S., Cai, D. S., Dyroff, C., Eckstein, J., Frank, F., Garny, H., Gottschaldt, K.-D., Graf, P., Grewe, V., Kerkweg, A., Kern, B., Matthes, S., Mertens, M., Meul, S., Neumaier, M., Nützel, M., Oberländer-Hayn, S., Ruhnke, R., Runde, T., Sander, R., Scharffe, D., and Zahn, A.: Earth System Chemistry integrated Modelling (ESCiMo) with the Modular Earth Submodel System (MESSy) version 2.51, Geosci. Model Dev., 9, 1153–1200, doi:10.5194/gmd-9-1153-2016, http://www.geosci-model-dev.net/9/1153/2016/, 2016.

Kalabokas, P., Mihalopoulos, N., Ellul, R., Kleanthous, S., and Repapis, C.: An investigation of the meteorological and photochemical factors influencing the background rural and marine surface ozone levels in the Central and Eastern Mediterranean, Atmos. Environ., 42, 7894–7906, doi:10.1016/j.atmosenv.2008.07.009, http://www.sciencedirect.com/science/article/pii/S1352231008006407, 2008.

Kalabokas, P. D., Volz-Thomas, A., Brioude, J., Thouret, V., Cammas, J.-P., and Repapis, C. C.: Vertical ozone measurements in the troposphere over the Eastern Mediterranean and comparison with Central Europe, Atmos. Chem. Phys., 7, 3783–3790, doi:10.5194/acp-7-3783-2007, http://www.atmos-chem-phys.net/7/3783/2007/, 2007.

Kalabokas, P. D., Cammas, J.-P., Thouret, V., Volz-Thomas, A., Boulanger, D., and Repapis, C. C.: Examination of the atmospheric conditions associated with high and low summer ozone levels in the lower troposphere over the eastern Mediterranean, Atmos. Chem. Phys., 13, 10 339–10 352, doi:10.5194/acp-13-10339-2013, http://www.atmos-chem-phys.net/13/10339/2013/, 2013.

Kesselmeier, J. and Staudt, M.: Biogenic Volatile Organic Compounds (VOC): An Overview on Emission, Physiology and Ecology, J. Atmos. Chem., 33, 23–88, doi:10.1023/A:1006127516791, http://dx.doi.org/10.1023/A%3A1006127516791, 1999.

Kesselmeier, J., Schäfer, L., Ciccioli, P., Brancaleoni, E., Cecinato, A., Frattoni, M., Foster, P., Jacob, V., Denis, J., Fugit, J., Dutaur, L., and Torres, L.: Emission of monoterpenes and isoprene from a Mediterranean oak species Quercus ilex L. measured within the BEMA (Biogenic Emissions in the Mediterranean Area) project, Atmos. Environ., 30, 1841–1850, doi:10.1016/1352-2310(95)00376-2, http://www.sciencedirect.com/science/article/pii/1352231095003762, 1996.

Kesselmeier, J., Bode, K., Schäfer, L., Schebeske, G., Wolf, A., Brancaleoni, E., Cecinato, A., Ciccioli, P., Frattoni, M., Dutaur, L., Fugit, J. L., Simon, V., and Torres, L.: Simultaneous field measurements of terpene and isoprene emissions from two dominant Mediterranean oak species in relation to a North American

species, Atmos. Environ., 32, 1947–1953, doi:10.1016/S1352-2310(97)00500-1, http://www.sciencedirect.com/science/article/pii/S1352231097005001, 1998.

Khan, M., Cooke, M., Utembe, S., Archibald, A., Maxwell, P., Morris, W., Xiao, P., Derwent, R., Jenkin, M., Percival, C., Walsh, R., Young, T., Simmonds, P., Nickless, G., O'Doherty, S., and Shallcross, D.: A study of global atmospheric budget and distribution of acetone using global atmospheric model STOCHEM-CRI, Atmos. Environ., 112, 269–277, doi:http://dx.doi.org/10.1016/j.atmosenv.2015.04.056, http://www.sciencedirect.com/science/article/pii/S1352231015300595, 2015.

Kleanthous, S., Vrekoussis, M., Mihalopoulos, N., Kalabokas, P., and Lelieveld, J.: On the temporal and spatial variation of ozone in Cyprus, Sci. total Environ., 476–477, 677–687, doi:10.1016/j.scitotenv.2013.12.101, http://www.sciencedirect.com/science/article/pii/S0048969713015842, 2014.

Kourtidis, K., Zerefos, C., Rapsomanikis, S., Simeonov, V., Balis, D., Perros, P. E., Thompson, A. M., Witte, J., Calpini, B., Sharobiem, W. M., Papayannis, A., Mihalopoulos, N., and Drakou, R.: Regional levels of ozone in the troposphere over eastern Mediterranean, J. Geophys. Res., 107, doi:10.1029/2000JD000140, http://dx.doi.org/10.1029/2000JD000140, 2002.

Kouvarakis, G., Vrekoussis, M., Mihalopoulos, N., Kourtidis, K., Rappenglueck, B., Gerasopoulos, E., and Zerefos, C.: Spatial and temporal variability of tropospheric ozone (O3) in the boundary layer above the Aegean Sea (eastern Mediterranean), J. Geophys. Res., 107, doi:10.1029/2000JD000081, http://dx.doi.org/10.1029/2000JD000081, 2002.

Lelieveld, J., Berresheim, H., Borrmann, S., Crutzen, P. J., Dentener, F. J., Fischer, H., Feichter, J., Flatau, P. J., Heland, J., Holzinger, R., Korrmann, R., Lawrence, M. G., Levin, Z., Markowicz, K. M., Mihalopoulos, N., Minikin, A., Ramanathan, V., de Reus, M., Roelofs, G. J., Scheeren, H. A., Sciare, J., Schlager, H., Schultz, M., Siegmund, P., Steil, B., Stephanou, E. G., Stier, P., Traub, M., Warneke, C., Williams, J., and Ziereis, H.: Global Air Pollution Crossroads over the Mediterranean, Science, 298, 794–799, doi:10.1126/science.1075457, http://dx.doi.org/10.1126/science.1075457, 2002.

Lelieveld, J., Gromov, S., Pozzer, A., and Taraborrelli, D.: Global tropospheric hydroxyl distribution, budget and reactivity, Atmos. Chem. Phys. Discuss., 2016, 1–25, doi:10.5194/acp-2016-160, http://www.atmos-chem-phys-discuss.net/acp-2016-160/, 2016.

Li, J., Parchatka, U., Königstedt, R., and Fischer, H.: Real-time measurements of atmospheric CO using a continuous-wave room temperature quantum cascade laser based spectrometer, Opt. Express, 20, 7590–7601, doi:10.1364/OE.20.007590, http://www.opticsexpress.org/abstract.cfm?URI=oe-20-7-7590, 2012.

Liakakou, E., Vrekoussis, M., Bonsang, B., Donousis, C., Kanakidou, M., and Mihalopoulos, N.: Isoprene above the Eastern Mediterranean: Seasonal variation and contribution to the oxidation capacity of the atmosphere, Atmos. Environ., 41, 1002–1010, doi:10.1016/j.atmosenv.2006.09.034, http://www.sciencedirect.com/science/article/pii/S1352231006009721, 2007.

Martinez, M., Harder, H., Kubistin, D., Rudolf, M., Bozem, H., Eerdekens, G., Fischer, H., Klüpfel, T., Gurk, C., Königstedt, R., Parchatka, U., Schiller, C. L., Stickler, A., Williams, J., and Lelieveld, J.: Hydroxyl radicals in the tropical troposphere over the Suriname rainforest: airborne measurements, Atmos. Chem. Phys., 10, 3759–3773, doi:10.5194/acp-10-3759-2010, http://www.atmos-chem-phys.net/10/3759/2010/, 2010.

Mesarchaki, E., Yassaa, N., D., H., Lutterbeck, H. E., Zindler, C., and Williams, J.: A novel method for the measurement of VOCs in seawater using needle trap devices and GC–MS, Mar.

Chem., 149, 1–8, doi:10.1016/j.marchem.2013.12.001, http://www.sciencedirect.com/science/article/pii/S0304420313002077, 2014.

Millet, D. B., Jacob, D. J., Custer, T. G., de Gouw, J. A., Goldstein, A. H., Karl, T., Singh, H. B., Sive, B. C., Talbot, R. W., Warneke, C., and Williams, J.: New constraints on terrestrial and oceanic sources of atmospheric methanol, Atmos. Chem. Phys., 8, 6887–6905, doi:10.5194/acp-8-6887-2008, http://www.atmos-chem-phys.net/8/6887/2008/, 2008.

Müller, J., Liu, Z., Nguyen, V. S., Stavrakou, T., Harvey, J. N., and Peeters, J.: The reaction of methyl peroxy and hydroxyl radicals as a major source of atmospheric methanol, Nature Communications, 7, 13 213, doi:10.1038/ncomms13213, http://search.proquest.com/docview/1829500178?accountid=104641, 2016.

Müller, M., Mikoviny, T., Jud, W., D'Anna, B., and Wisthaler, A.: A new software tool for the analysis of high resolution PTR-TOF mass spectra, Chemometrics Intell. Lab. Sys., 127, 158–165, doi:10.1016/j.chemolab.2013.06.011, http://www.sciencedirect.com/science/article/pii/S0169743913001275, 2013.

Niki, H., Maker, P. D., Savage, C. M., and Breitenbach, L. P.: An FTIR study of mechanisms for the HO radical initiated oxidation of C2H4 in the presence of NO: detection of glycolaldehyde, Chem. Phys. Lett., 80, 1981.

Novelli, A., Hens, K., Tatum Ernest, C., Kubistin, D., Regelin, E., Elste, T., Plass-Dülmer, C., Martinez, M., Lelieveld, J., and Harder, H.: Characterisation of an inlet pre-injector laser-induced fluorescence instrument for the measurement of atmospheric hydroxyl radicals, Atmos. Meas. Tech., 7, 3413–3430, doi:10.5194/amt-7-3413-2014, http://www.atmos-meas-tech.net/7/3413/2014/, 2014.

Owen, S. M., Harley, P., Guenther, A., and Hewitt, C. N.: Light dependency of {VOC} emissions from selected Mediterranean plant species, Atmos. Environ., 36, 3147 – 3159, doi:10.1016/S1352-2310(02)00235-2, //www.sciencedirect.com/science/article/pii/S1352231002002352, 2002.

Palmer, P. I. and Shaw, S. L.: Quantifying global marine isoprene fluxes using MODIS chlorophyll observations, Geophys. Res. Lett., 32, doi:10.1029/2005GL022592, http://dx.doi.org/10.1029/2005GL022592, 2005.

Paulot, F., Wunch, D., Crounse, J. D., Toon, G. C., Millet, D. B., DeCarlo, P. F., Vigouroux, C., Deutscher, N. M., González Abad, G., Notholt, J., Warneke, T., Hannigan, J. W., Warneke, C., de Gouw, J. A., Dunlea, E. J., De Mazière, M., Griffith, D. W. T., Bernath, P., Jimenez, J. L., and Wennberg, P. O.: Importance of secondary sources in the atmospheric budgets of formic and acetic acids, Atmos. Chem. Phys., 11, 1989–2013, doi:10.5194/acp-11-1989-2011, www.atmos-chem-phys.net/11/1989/2011/, 2011.

Paulson, S. E. and Seinfeld, J. H.: Development and Evaluation of a Photooxidation Mechanism for Isoprene, J. Geophys. Res., 97, 20, 703–20,715, 1992.

Phillips, G. J., Pouvesle, N., Thieser, J., Schuster, G., Axinte, R., Fischer, H., Williams, J., Lelieveld, J., and Crowley, J. N.: Peroxyacetyl nitrate (PAN) and peroxyacetic acid (PAA) measurements by iodide chemical ionisation mass spectrometry: first analysis of results in the boreal forest and implications for the measurement of PAN fluxes, Atmos. Chem. Phys., 13, 1129–1139, doi:10.5194/acp-13-1129-2013, http://www.atmos-chem-phys.net/13/1129/2013/, 2013.

Salisbury, G., Williams, J., Holzinger, R., Gros, V., Mihalopoulos, N., Vrekoussis, M., Sarda-Estève, R., Berresheim, H., von Kuhlmann, R., Lawrence, M., and Lelieveld, J.: Ground-based PTR-MS measurements of reactive organic compounds during the MINOS campaign in Crete, July–August 2001, Atmos. Chem. Phys., 3, 925–940, doi:10.5194/acp-3-925-2003, http://www.atmos-chem-phys.net/3/925/2003/, 2003.

Sander, R.: Compilation of Henry's law constants (version 4.0) for water as solvent, Atmos. Chem. Phys., 15, 4399–4981, doi:10.5194/acp-15-4399-2015, http://www.atmos-chem-phys.net/15/4399/2015/, 2015.

Sander, R., Baumgaertner, A., Gromov, S., Harder, H., Jöckel, P., Kerkweg, A., Kubistin, D., Regelin, E., Riede, H., Sandu, A., Taraborrelli, D., Tost, H., and Xie, Z.-Q.: The atmospheric chemistry box model CAABA/MECCA-3.0, Geosci. Model Dev., 4, 373–380, doi:10.5194/gmd-4-373-2011, http://www.geosci-model-dev.net/4/373/2011/, 2011.

Sinha, V., Williams, J., Meyerhöfer, M., Riebesell, U., Paulino, A. I., and Larsen, A.: Air-sea fluxes of methanol, acetone, acetaldehyde, isoprene and DMS from a Norwegian fjord following a phytoplankton bloom in a mesocosm experiment, Atmos. Chem. Phys., 7, 739–755, doi:10.5194/acp-7-739-2007, http://www.atmos-chem-phys.net/7/739/2007/, 2007.

Spanel, P., Diskin, A., Wang, T., and Smith, D.: A SIFT study of the reactions of $H_3O^+$, $NO^+$, and $O_2^+$ with hydrogen peroxide and peroxyacetic acid, Int. J. Mass Spectrom., 228, 269–283, doi:10.1016/S1387-3806(03)00214-8, http://www.sciencedirect.com/science/article/pii/S1387380603002148, 2003.

Staudt, M., Bertin, N., Hansen, U., Seufert, G., Cicciolij, P., Foster, P., Frenzel, B., and Fugit, J.-L.: Seasonal and diurnal patterns of monoterpene emissions from Pinus pinea (L.) under field conditions, Atmos. Environ., 31, 145–156, doi:10.1016/S1352-2310(97)00081-2, http://www.sciencedirect.com/science/article/pii/S1352231097000812, 1997.

Stohl, A., Eckhardt, S., Forster, C., James, P., Spichtinger, N., and Seibert, P.: A replacement for simple back trajectory calculations in the interpretation of atmospheric trace substance measurements, Atmos. Environ., 36, 4635–4648, doi:10.1016/S1352-2310(02)00416-8, http://www.sciencedirect.com/science/article/pii/S1352231002004168, 2002.

Stohl, A., Forster, C., Frank, A., Seibert, P., and Wotawa, G.: Technical note: The Lagrangian particle dispersion model FLEXPART version 6.2, Atmos. Chem. Phys., 5, 2461–2474, doi:10.5194/acp-5-2461-2005, http://www.atmos-chem-phys.net/5/2461/2005/, 2005.

Stohl, A., Berg, T., Burkhart, J. F., Fjæraa, A. M., Forster, C., Herber, A., Hov, Ø., Lunder, C., McMillan, W. W., Oltmans, S., Shiobara, M., Simpson, D., Solberg, S., Stebel, K., Ström, J., Tørseth, K., Treffeisen, R., Virkkunen, K., and Yttri, K. E.: Arctic smoke — record high air pollution levels in the European Arctic due to agricultural fires in Eastern Europe in spring 2006, Atmos. Chem. Phys., 7, 511–534, doi:10.5194/acp-7-511-2007, http://www.atmos-chem-phys.net/7/511/2007/, 2007.

Taddei, S., Toscano, P., Gioli, B., Matese, A., Miglietta, F., Vaccari, F. P., Zaldei, A., Custer, T., and Williams, J.: Carbon Dioxide and Acetone Air Sea Fluxes over the Southern Atlantic, Environ. Sci. Technol., 43, 5218–5222, doi:10.1021/es8032617, http://dx.doi.org/10.1021/es8032617, 2009.

Tyrlis, E., Tymvios, F. S., Giannakopoulos, C., and Lelieveld, J.: The role of blocking in the summer 2014 collapse of Etesians over the eastern Mediterranean, J. Geophys. Res. - Atmos., 120, 6777–6792, doi:10.1002/2015JD023543, http://dx.doi.org/10.1002/2015JD023543, 2015.

Veres, P. R., Faber, P., Drewnick, F., Lelieveld, J., and Williams, J.: Anthropogenic sources of VOC in a football stadium: Assessing human emissions in the atmosphere, Atmos. Environ., 77, 1052–1059, doi:10.1016/j.atmosenv.2013.05.076, http://www.sciencedirect.com/science/article/pii/S1352231013004494, 2013.

Warneke, C., van der Veen, C., Luxembourg, S., de Gouw. J. A., and Kok, A.: Measurements of benzene and toluene in ambient air using proton-transfer-reaction mass spectrometry: calibration, humidity dependence, and field intercomparison, Int. J. Mass Spectrom., 207, 167 – 182, doi:10.1016/S1387-3806(01)00366-9, //www.sciencedirect.com/science/article/pii/S1387380601003669, 2001.

Williams, J., Holzinger, R., Gros, V., Xu, X., Atlas, E., and Wallace, D. W. R.: Measurements of organic species in air and seawater from the tropical Atlantic, Geophys. Res. Lett., 31, doi:10.1029/2004GL020012, http://dx.doi.org/10.1029/2004GL020012, 2004.

Xu, X., Stee, L. L. P., Williams, J., Beens, J., Adahchour, M., Vreuls, R. J. J., Brinkman, U. A., and Lelieveld, J.: Comprehensive two-dimensional gas chromatography (GC × GC) measurements of volatile organic compounds in the atmosphere, Atmos. Chem. Phys., 3, 665–682, doi:10.5194/acp-3-665-2003, http://www.atmos-chem-phys.net/3/665/2003/, 2003.

Yañez Serrano, A. M., Nölscher, A. C., Williams, J., Wolff, S., Alves, E., Martins, G. A., Bourtsoukidis, E., Brito, J., Jardine, K., Artaxo, P., and Kesselmeier, J.: Diel and seasonal changes of biogenic volatile organic compounds within and above an Amazonian rainforest, Atmos. Chem. Phys., 15, 3359–3378, doi:10.5194/acp-15-3359-2015, http://www.atmos-chem-phys.net/15/3359/2015/acp-15-3359-2015.html, 2015.

Yang, M., Nightingale, P. D., Beale, R., Liss, P. S., Blomquist, B., and Fairall, C.: Atmospheric deposition of methanol over the Atlantic Ocean, Proc. Natl. Acad. Sci. USA, 110, 20 034–20 039, doi:10.1073/pnas.1317840110, http://www.pnas.org/content/110/50/20034.abstract, 2013.

Yang, M., Beale, R., Liss, P., Johnson, M., Blomquist, B., and Nightingale, P.: Air–sea fluxes of oxygenated volatile organic compounds across the Atlantic Ocean, Atmos. Chem. Phys., 14, 7499–7517, doi:10.5194/acp-14-7499-2014, http://www.atmos-chem-phys.net/14/7499/2014/, 2014.

Yassaa, N., Song, W., Lelieveld, J., Vanhatalo, A., Bäck, J., and Williams, J.: Diel cycles of isoprenoids in the emissions of Norway spruce, four Scots pine chemotypes, and in Boreal forest ambient air during HUMPPA-COPEC-2010, Atmos. Chem. Phys., 12, 7215–7229, doi:10.5194/acp-12-7215-2012, http://www.atmos-chem-phys.net/12/7215/2012/, 2012.

**Table 1.** Averaged data of VOCs, $O_3$ and CO and their standard deviation in pptv ~~for~~ based on a 10 min time resolution. The data were separated into periods reached by air from eastern or western regions ~~. For~~ as well as into values measured when the ~~calculation only data above~~ site was within the ~~detection limit~~ residual layer/free troposphere (~~3 σ~~RL/FT) ~~were used~~ and ~~n represents~~ those recorded when the ~~number of points above this limit~~site was within the PBL.

| Compound | ~~Eastern air~~ East ~~mass~~ RL/FT | ~~Standard~~ Std. dev. ~~deviation (east )~~east RL/FT | ~~Western air~~ West ~~mass~~ RL/FT | ~~Standard~~ Std. dev. ~~deviation (west )~~ west RL |
|---|---|---|---|---|
| Methanol | ~~3545 (n = 1687)~~ 4389 | ~~949~~ 866 | ~~2571 (n = 908)~~ 3251 | ~~694~~ 241 |
| Acetonitrile | ~~112 (n = 1695)~~132 | ~~23~~ 19 | ~~108 (n = 908)~~ 147 | ~~29~~ 22 |
| Acetaldehyde | ~~370 (n = 1625)~~ 345 | ~~146~~ 112 | ~~246 (n = 907)~~ 190 | ~~92~~ 33 |
| Acetone | ~~2659 (n = 1695)~~ 3158 | ~~576~~ 694 | ~~1994 (n = 908)~~ 2099 | ~~342~~ 157 |
| Acetic acid | ~~1280 (n = 1566)~~ 1709 | ~~598~~ 681 | ~~778 (n = 851)~~ 1039 | ~~312 Dimethylsulfide~~ 16 |
| Isoprene | ~~101 (n = 941)~~15 | ~~62~~ 16 | ~~78 (n = 498)~~ 3 | 4 |
| Methylvinylketone Methacrolein/ISOPOOH | ~~43 (n = 910)~~ 9 | 7 | 4 | 3 |
| Methylethylketone | ~~127 (n = 1695)~~ 124 | ~~32~~ 40 | ~~81 (n = 908)~~ 44 | ~~21~~ 10 |
| Benzene | ~~37 (n = 1515)~~ 34 | ~~16~~ 19 | ~~24 (n = 230)~~ 13 | ~~11~~ 3 |
| Toluene | ~~19 (n = 462)~~ 5 | ~~21~~ 3 | ~~17 (n = 72)~~ 2 | ~~7~~ 2 |
| Total xylenes | ~~26 (n = 427)~~ 7 | ~~33~~ 5 | ~~49 (n = 99)~~ 4 | ~~124~~ 4 |
| Total trimethylbenzenes | ~~19 (n = 223)~~ 5 | ~~29~~ 3 | ~~27 (n = 96)~~ 2 | ~~74~~ 2 |
| Total monoterpenes | ~~65 (n = 1326)~~ 11 | ~~56~~ 14 | ~~49 (n = 736)~~ 4 | 2 |
| Ozone | ~~73588 (n = 2036)~~ 82364 | ~~9441~~ 9911 | ~~61844 (n = 994)~~ 73096 | ~~8627~~ 5771 |
| ~~CO~~ Carbonmonoxide | ~~107274 (n = 2054)~~ 110522 | ~~9868~~ 11497 | ~~91361 (n = 1003)~~ 95484 | ~~6902~~ 7914 |

**Table 2.** Slope, intercept and correlation coefficient ($r^2$) of different compounds separated in air masses from Eastern and Western Europe

| | |
|---|---|
| | ~~$slope = 1.8, intercept = -1.1, r^2 = 0.76$~~ ~~$slope = 2.8, intercept = -3.0, r^2 = 0.62$~~ |
| | |
| | |
| | |
| ~~$slope = 0.046, intercept = -2.3, r^2 = 0.61$~~ ~~$slope = 0.030, intercept = -0.80, r^2 = 0.52$~~Acetic acid vs. ozone Acetic acid vs. ozone ~~$slope =$~~ | |

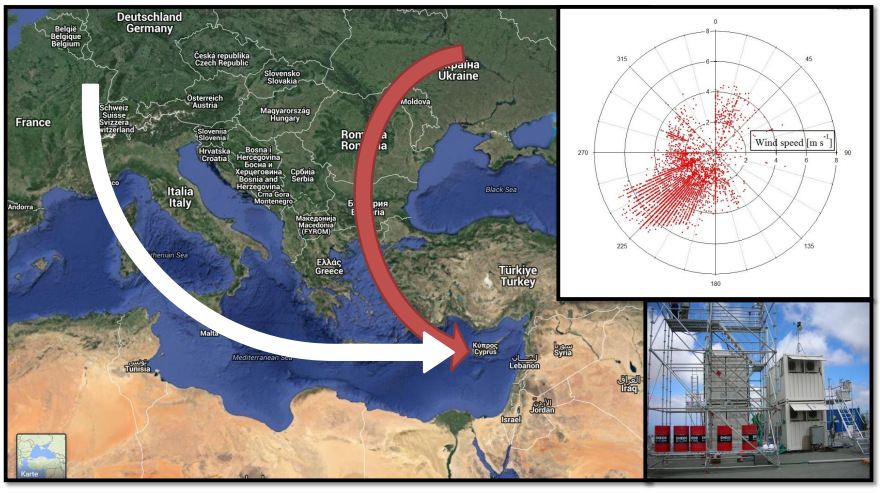


**Figure 1.** Map of the Mediterranean basin (Source: Google). The white arrow shows the inflow from Western and the red the inflow from Eastern Europe. On the right hand side a wind rose displaying the dominant wind direction and a picture of the laboratory containers can be seen.

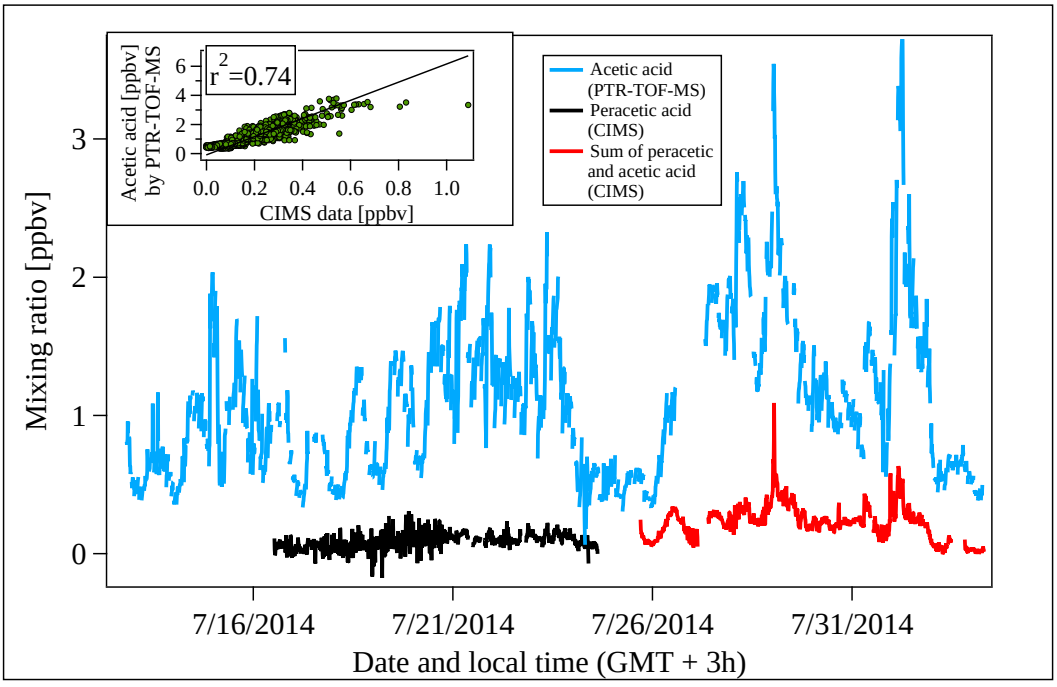


**Figure 2.** Time traces of peracetic acid (black) and the sum of peracetic and acetic acid (red) measured by CIMS ~~and~~ as well as acetic acid measured by PTR-TOF-MS (10 min mean values). The upper left plot shows the correlation between ~~both compounds~~ PTR-TOF-MS and CIMS data from 26 July until the end of the campaign.

~~Box and whiskers plots~~

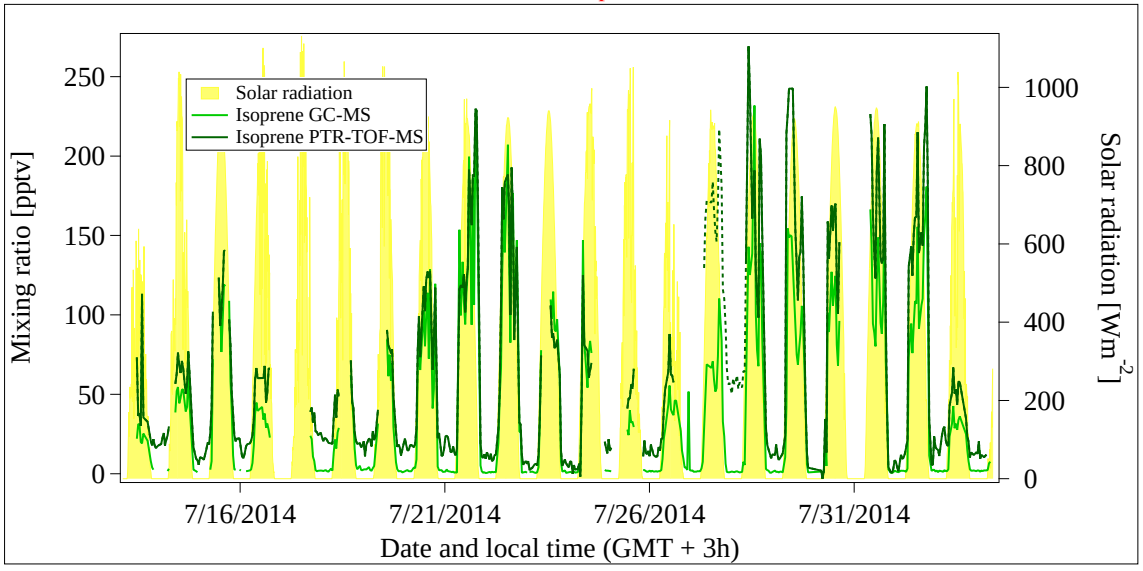


**Figure 3.** Time traces of isoprene in pptv measured by GC-MS and ~~the sum of monoterpenes~~PTR-TOF-MS as well as solar radiation in $Wm^{-2}$. The ~~box contains 50 % of the~~ PTR-TOF-MS data ~~. 25 %~~ with a time resolution of 1 min were merged on the ~~data lie below the lower end~~ 20 minute sampling time of the ~~box, 75 % below the upper end~~GC-MS. Solar radiation is shown in a 10 min time resolution. The ~~whiskers present the 5–95 % range of~~ dashed line marks a possible contamination in the PTR-TOF-MS data.

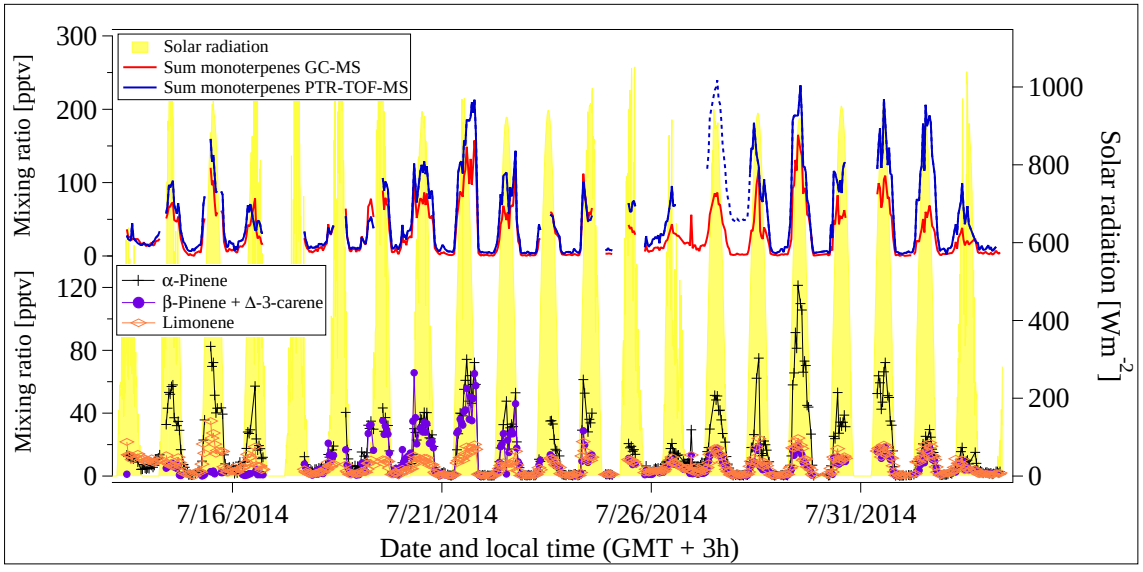


**Figure 4.** Time traces of ~~isoprene and~~ different monoterpenes in pptv ~~measured by GC-MS~~ as well as solar radiation in $Wm^{-2}$. The PTR-TOF-MS data with a time resolution of 1 min were merged on the 20 minute sampling time of the GC-MS. Solar radiation is shown in a 10 min time resolution. The upper part shows the sum of the monoterpenes measured by GC-MS and PTR-TOF-MS, the lower part displays individual monoterpenes measured by GC-MS, only. The dashed line marks a possible contamination in the PTR-TOF-MS data.

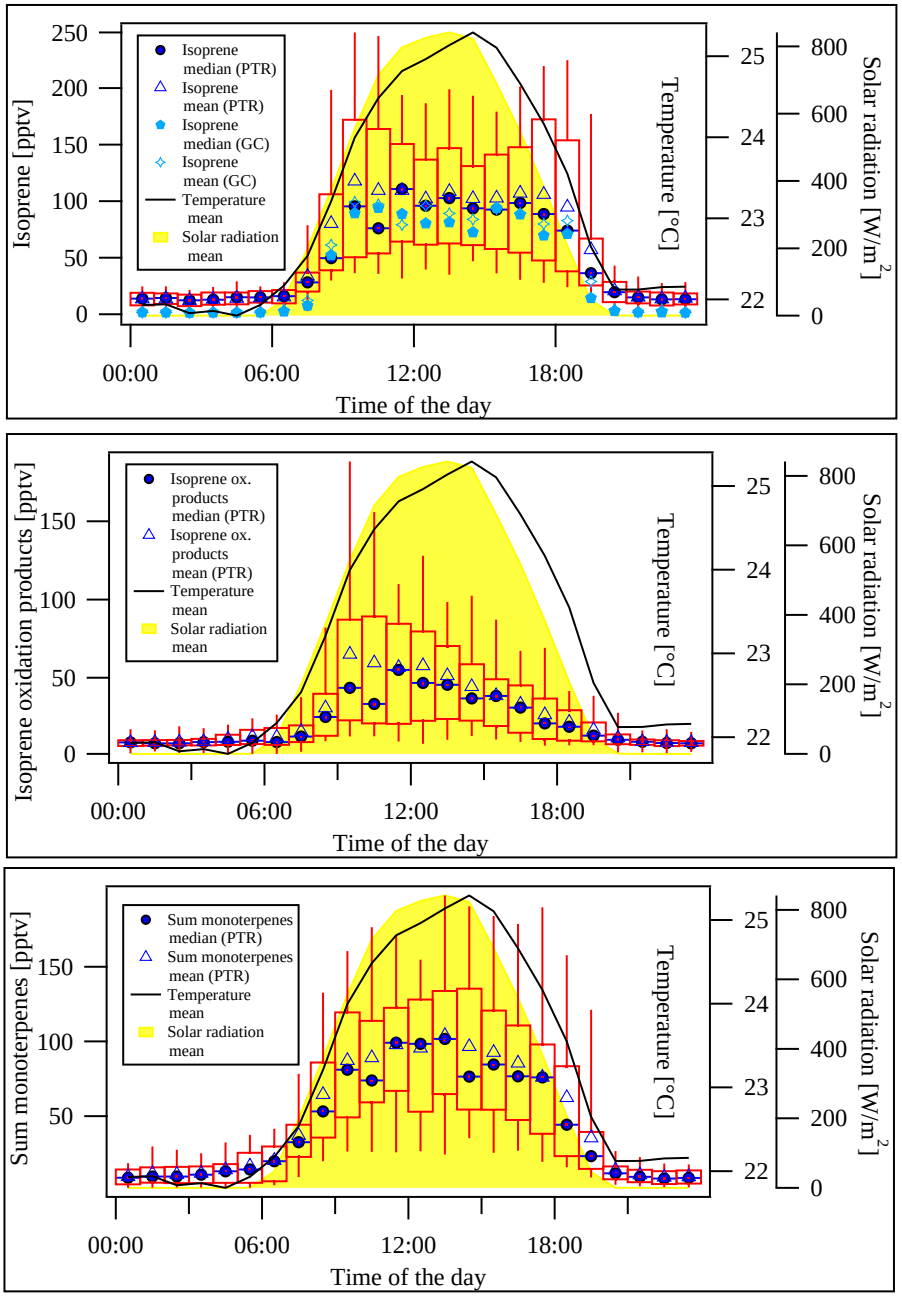


**Figure 5.** Box and whiskers plots of isoprene, the oxidations products of isoprene and the sum of monoterpenes for the whole campaign with a 1 h time resolution as measured by the PTR-TOF-MS. For comparison the median and mean isoprene values measured by GC-MS were added in the upper panel. To calculate the boxplots PTR-TOF-MS data with a time resolution of 10 min and GC-MS data with a 45 min time resolution (20 min sampling time) were used. The contaminations in isoprene and the monoterpenes determined by comparing GC-MS and PTR-TOF-MS data were cut. The box contains 50 % of the data. 25 % of the data lie below the lower end of the box, 75 % below the upper end. The whiskers present the 5–95 % range of the data.

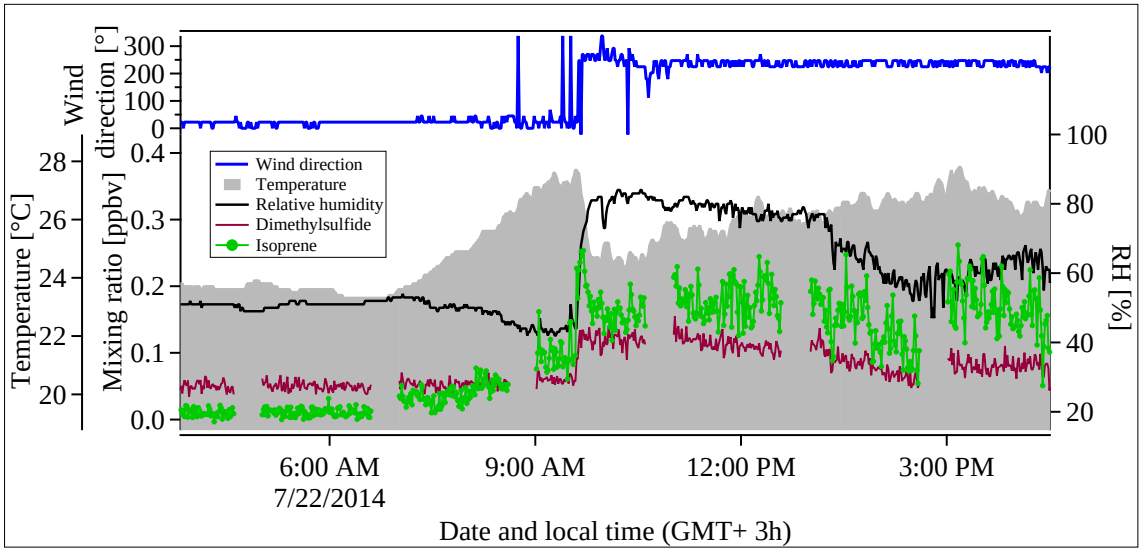


**Figure 6.** Mixing ratios of isoprene and DMS in ppbv as well as wind direction in °, temperature in °C and relative humidity in % as a function of time with ~~an one~~ a 1 minute time resolution.

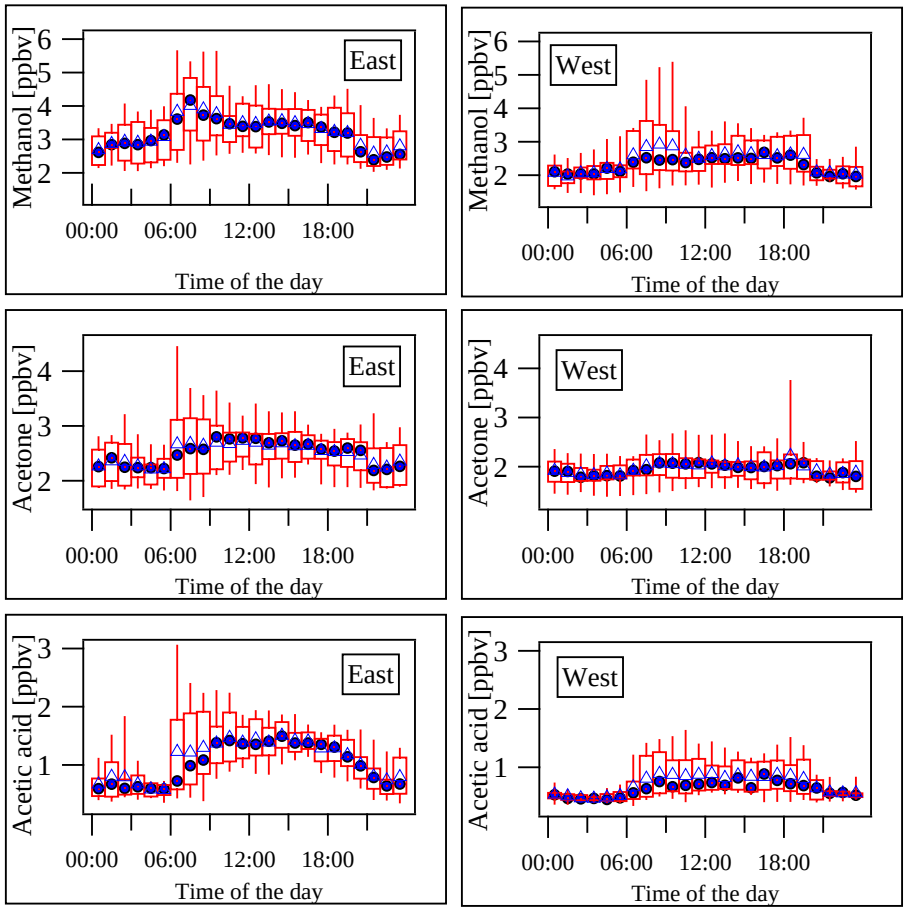


**Figure 7.** Box and whiskers plot of acetone, methanol and acetic acid when the site was within the PBL. The triangles refer to mean and the circles to median values. The box contains 50 % of the data. 25 % of the data lie below the lower end of the box, 75 % below the upper end. The whiskers present the 5–95 % range of the data.

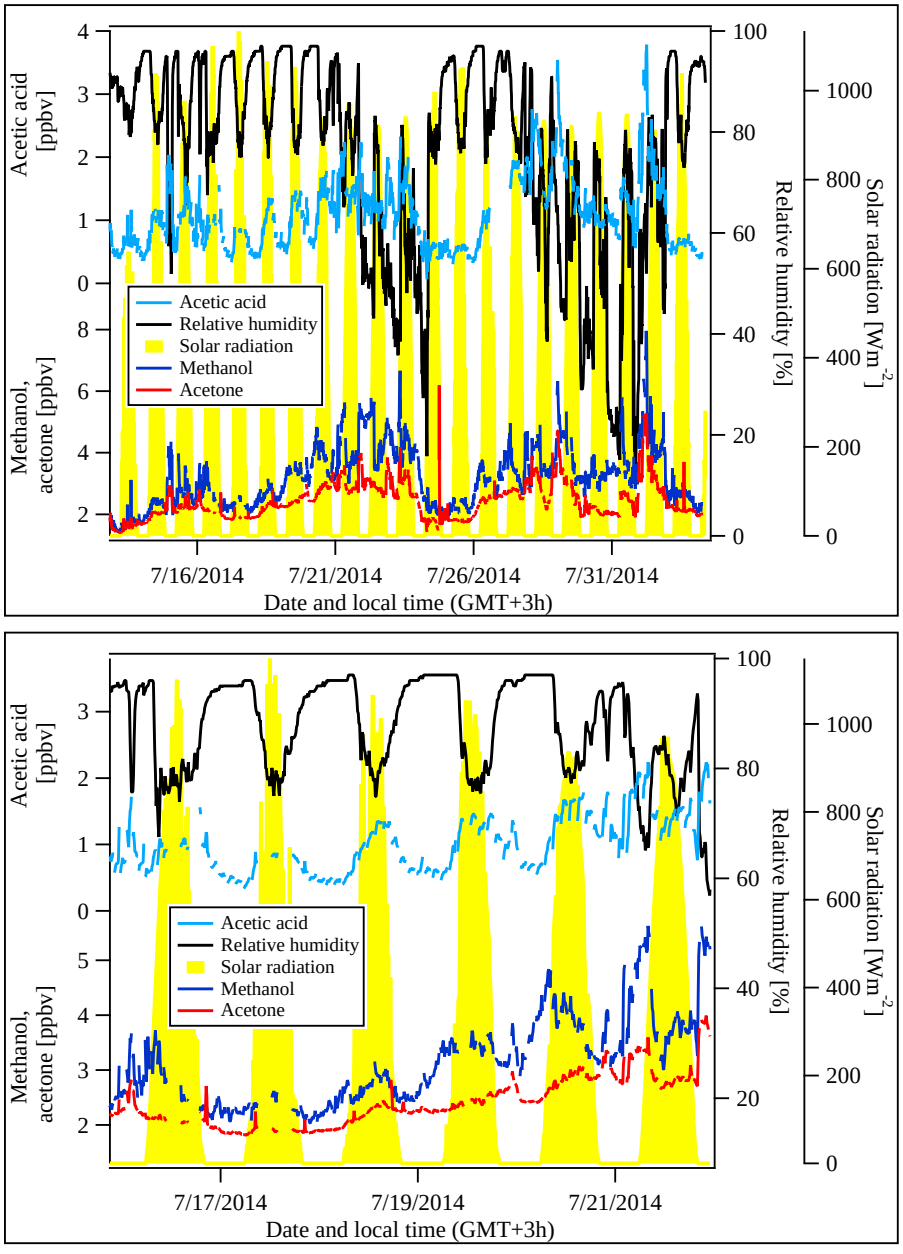


**Figure 8.** Mixing ratios of acetic acid, acetone and methanol in ppbv~~(10 min mean values)~~, relative humidity in % and solar radiation in $Wm^{-2}$ (10 min mean values) as a function of time. The lower panel ~~shows~~ is a ~~detail~~ zoom in from 16 to 21 July.

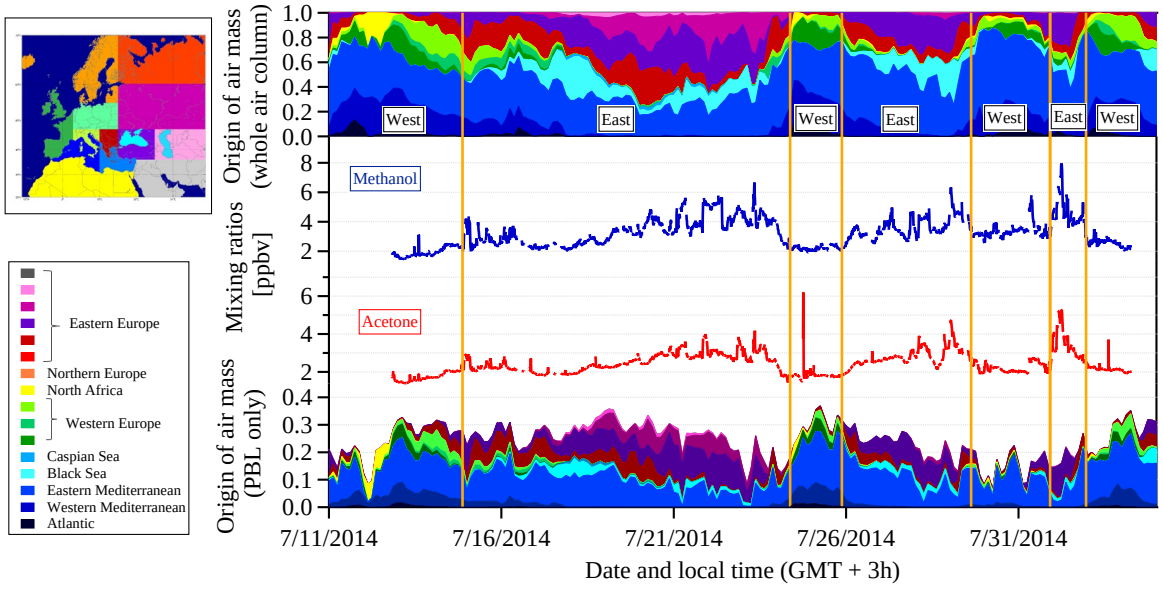


**Figure 9.** Allocation of Europe into specific regions (upper left panel) as well as traces of methanol ~~, acetone~~ and ~~acetic acid~~ acetone in ppbv (10 min mean values) and modeled data of the area of influence, given in fractions of 1. The upper part of the right panel refers to the whole air column, while the lower part of the right panel represents the PBL, only.

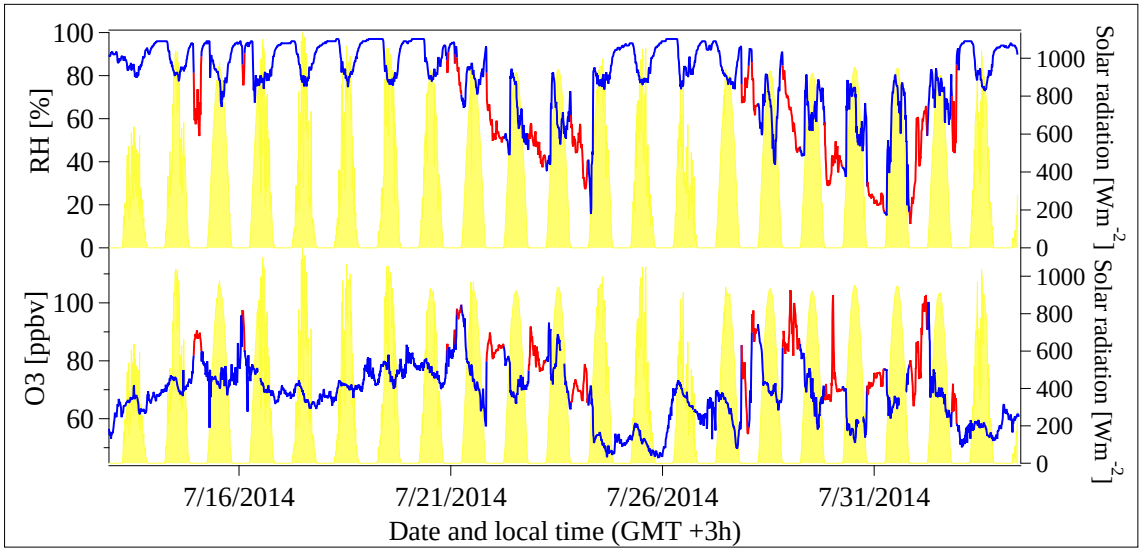


**Figure 10.** Ozone in ppbv, relative humidty in % and solar radiation in $Wm^{-2}$ (10 min mean values). The red data points are influenced by air masses from the residual layer/free troposphere.

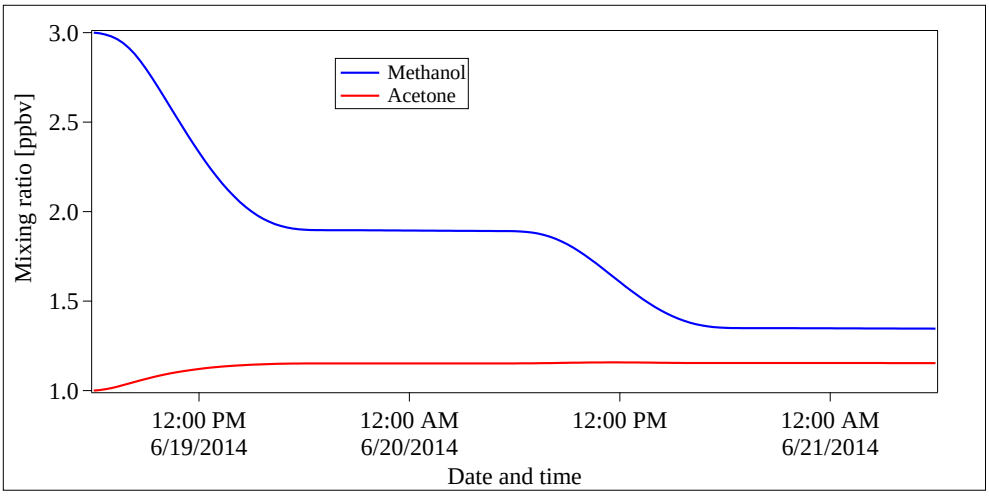


**Figure 11.** Modeled mixing ratios of ~~acetic acid, acetone and~~ methanol and acetone in ppbv over the period of 48 h starting at 6 am. Initial values originate from the MOM chemistry in the global model EMAC (Jöckel et al., 2016).

~~Rates for reactions influencing the mixing ratio of methanol. Further explanation of the reactions can be found in the supplement.~~

~~Rates for reactions influencing the mixing ratio of acetone. Further explanation of the reactions can be found in the supplement.~~

~~Rates for reactions influencing the mixing ratio of acetic acid. Further explanation of the reactions can be found in the supplement.~~

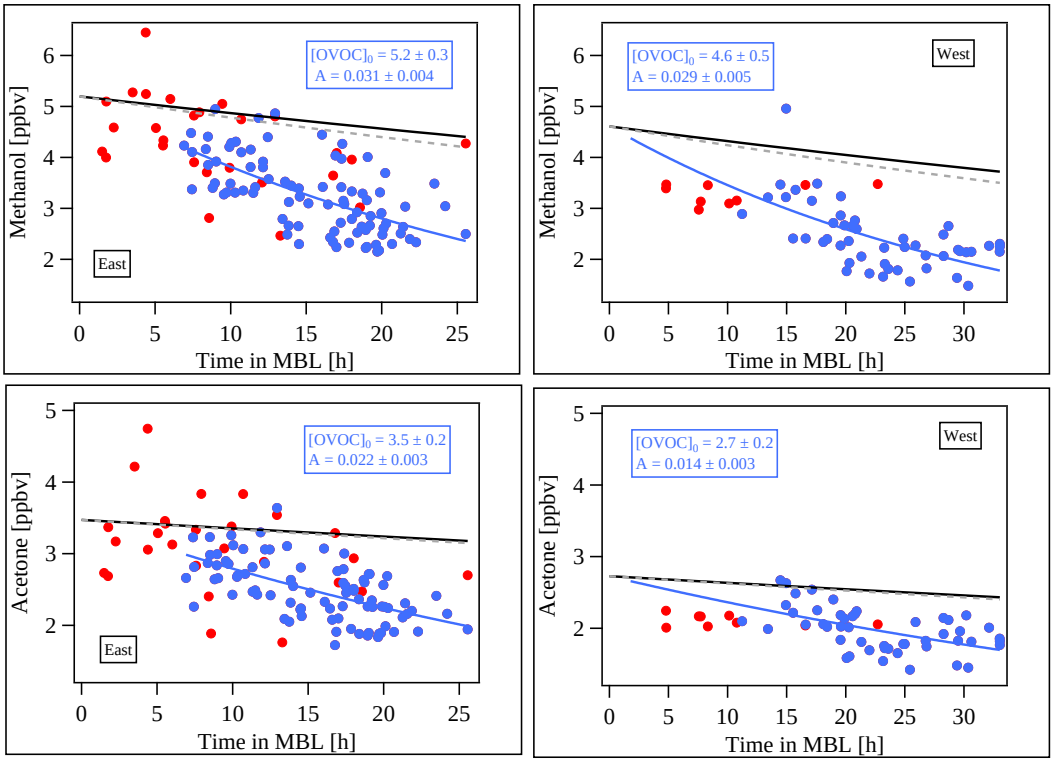


**Figure 12.** Data of acetone ~~, methanol~~ and ~~acetic acid~~ methanol separated by eastern and western air masses, plotted against the time in the MBL. The data measured within the PBL (marked in blue) were fitted using ~~a linear~~ an exponential fit algorithm (~~black~~ blue line). The ~~light blue~~ black lines refer to calculated ~~loss rates~~ losses using equation 4 and the dry deposition ~~rates~~ velocities from the EMAC model. The ~~violet lines~~ gray dashed line was calculated using a 28.5 % higher OH concentration. The red marks represent ~~loss rates adjusted by solubility relative~~ data points measured when the site was within the residual layer/free troposphere. These were excluded for the calculation of the exponential fit. $[OVOC]_0$ and A refer to ~~methanol~~equation 3 and are given in units of ppbv and $h^{-1}$, respectively.

~~Correlations between the OVOCs separated by eastern and western flow regimes. A bivariate fitting method was applied.~~

~~Correlation plots exclusively from western air masses were color coded by ozone data and relative humidity to show different branches~~

~~Correlations plots solely from eastern flow regimes were color coded by ozone data~~